



National Library
of Canada

Acquisitions and
Bibliographic Services Branch

395 Wellington Street
Ottawa, Ontario
K1A 0N4

Bibliothèque nationale
du Canada

Direction des acquisitions et
des services bibliographiques

395, rue Wellington
Ottawa (Ontario)
K1A 0N4

Your file - Votre référence

Our file - Notre référence

NOTICE

The quality of this microform is heavily dependent upon the quality of the original thesis submitted for microfilming. Every effort has been made to ensure the highest quality of reproduction possible.

If pages are missing, contact the university which granted the degree.

Some pages may have indistinct print especially if the original pages were typed with a poor typewriter ribbon or if the university sent us an inferior photocopy.

Reproduction in full or in part of this microform is governed by the Canadian Copyright Act, R.S.C. 1970, c. C-30, and subsequent amendments.

AVIS

La qualité de cette microforme dépend grandement de la qualité de la thèse soumise au microfilmage. Nous avons tout fait pour assurer une qualité supérieure de reproduction.

S'il manque des pages, veuillez communiquer avec l'université qui a conféré le grade.

La qualité d'impression de certaines pages peut laisser à désirer, surtout si les pages originales ont été dactylographiées à l'aide d'un ruban usé ou si l'université nous a fait parvenir une photocopie de qualité inférieure.

La reproduction, même partielle, de cette microforme est soumise à la Loi canadienne sur le droit d'auteur, SRC 1970, c. C-30, et ses amendements subséquents.

Canada

**THERMAL PERFORMANCE OF A ROOM WITH
WALL LATENT HEAT STORAGE**

CHUNYAN LIU

A thesis

in

The Centre for Building Studies

Presented in Partial Fulfilment of the Requirements

for the Degree of Master of Applied Science

Concordia University

Montreal, Quebec, Canada

September 1993

©Chunyan Liu, 1993



National Library
of Canada

Acquisitions and
Bibliographic Services Branch

395 Wellington Street
Ottawa, Ontario
K1A 0N4

Bibliothèque nationale
du Canada

Direction des acquisitions et
des services bibliographiques

395, rue Wellington
Ottawa (Ontario)
K1A 0N4

Your file - Votre référence

Our file - Notre référence

The author has granted an irrevocable non-exclusive licence allowing the National Library of Canada to reproduce, loan, distribute or sell copies of his/her thesis by any means and in any form or format, making this thesis available to interested persons.

L'auteur a accordé une licence irrévocable et non exclusive permettant à la Bibliothèque nationale du Canada de reproduire, prêter, distribuer ou vendre des copies de sa thèse de quelque manière et sous quelque forme que ce soit pour mettre des exemplaires de cette thèse à la disposition des personnes intéressées.

The author retains ownership of the copyright in his/her thesis. Neither the thesis nor substantial extracts from it may be printed or otherwise reproduced without his/her permission.

L'auteur conserve la propriété du droit d'auteur qui protège sa thèse. Ni la thèse ni des extraits substantiels de celle-ci ne doivent être imprimés ou autrement reproduits sans son autorisation.

ISBN 0-315-90892-0

Canada

Name

CHUNYAN LIU

Dissertation Abstracts International is arranged by broad, general subject categories. Please select the one subject which most nearly describes the content of your dissertation. Enter the corresponding four-digit code in the spaces provided.

MECHANICAL

SUBJECT TERM

0548

U·M·I

SUBJECT CODE

Subject Categories

THE HUMANITIES AND SOCIAL SCIENCES

COMMUNICATIONS AND THE ARTS

Architecture	0729
Art History	0377
Cinema	0900
Dance	0378
Fine Arts	0357
Information Science	0723
Journalism	0391
Library Science	0399
Mass Communications	0708
Music	0413
Speech Communication	0459
Theater	0465

EDUCATION

General	0515
Administration	0514
Adult and Continuing	0516
Agricultural	0517
Art	0273
Bilingual and Multicultural	0262
Business	0688
Community College	0275
Curriculum and Instruction	0727
Early Childhood	0518
Elementary	0524
Finance	0277
Guidance and Counseling	0519
Health	0680
Higher	0745
History of	0520
Home Economics	0278
Industrial	0521
Language and Literature	0279
Mathematics	0280
Music	0522
Philosophy of	0998
Physical	0523

Psychology	0525
Reading	0535
Religious	0527
Sciences	0714
Secondary	0533
Social Sciences	0534
Sociology of	0340
Special	0529
Teacher Training	0530
Technology	0710
Tests and Measurements	0288
Vocational	0747

LANGUAGE, LITERATURE AND LINGUISTICS

Language	
General	0679
Ancient	0289
Linguistics	0290
Modern	0291
Literature	
General	0401
Classical	0294
Comparative	0295
Medieval	0297
Modern	0298
African	0316
American	0591
Asian	0305
Canadian (English)	0352
Canadian (French)	0355
English	0593
Germanic	0311
Latin American	0312
Middle Eastern	0315
Romance	0313
Slavic and East European	0314

PHILOSOPHY, RELIGION AND THEOLOGY

Philosophy	0422
Religion	
General	0318
Biblical Studies	0321
Clergy	0319
History of	0320
Philosophy of	0322
Theology	0469

SOCIAL SCIENCES

American Studies	0323
Anthropology	
Archaeology	0324
Cultural	0326
Physical	0327
Business Administration	
General	0310
Accounting	0272
Banking	0770
Management	0454
Marketing	0338
Canadian Studies	0385
Economics	
General	0501
Agricultural	0503
Commerce-Business	0505
Finance	0508
History	0509
Labor	0510
Theory	0511
Folklore	0358
Geography	0366
Gerontology	0351
History	
General	0578

Ancient	0579
Medieval	0581
Modern	0582
Black	0328
African	0331
Asia, Australia and Oceania	0332
Canadian	0334
European	0335
Latin American	0336
Middle Eastern	0333
United States	0337
History of Science	0585
Law	0398
Political Science	
General	0615
International Law and Relations	0616
Public Administration	0617
Recreation	0814
Social Work	0452
Sociology	
General	0626
Criminology and Penology	0627
Demography	0938
Ethnic and Racial Studies	0631
Individual and Family Studies	0628
Industrial and Labor Relations	0629
Public and Social Welfare	0630
Social Structure and Development	0700
Theory and Methods	0344
Transportation	0709
Urban and Regional Planning	0999
Women's Studies	0453

THE SCIENCES AND ENGINEERING

BIOLOGICAL SCIENCES

Agriculture	
General	0473
Agronomy	0285
Animal Culture and Nutrition	0475
Animal Pathology	0476
Food Science and Technology	0359
Forestry and Wildlife	0478
Plant Culture	0479
Plant Pathology	0480
Plant Physiology	0817
Range Management	0777
Wood Technology	0746
Biology	
General	0306
Anatomy	0287
Biostatistics	0308
Botany	0309
Cell	0379
Ecology	0329
Entomology	0353
Genetics	0369
Limnology	0793
Microbiology	0410
Molecular	0307
Neuroscience	0317
Oceanography	0416
Physiology	0433
Radiation	0821
Veterinary Science	0778
Zoology	0472
Biophysics	
General	0786
Medical	0760

EARTH SCIENCES

Biogeochemistry	0425
Geochemistry	0996

Geodesy	0370
Geology	0372
Geophysics	0373
Hydrology	0388
Mineralogy	0411
Paleobotany	0345
Paleoecology	0426
Paleontology	0418
Paleozoology	0985
Palynology	0427
Physical Geography	0368
Physical Oceanography	0415

HEALTH AND ENVIRONMENTAL SCIENCES

Environmental Sciences	0768
Health Sciences	
General	0566
Audiology	0300
Chemotherapy	0992
Dentistry	0567
Education	0350
Hospital Management	0769
Human Development	0758
Immunology	0982
Medicine and Surgery	0564
Mental Health	0347
Nursing	0569
Nutrition	0570
Obstetrics and Gynecology	0380
Occupational Health and Therapy	0354
Ophthalmology	0381
Pathology	0571
Pharmacology	0419
Pharmacy	0572
Physical Therapy	0382
Public Health	0573
Radiology	0574
Recreation	0575

Speech Pathology	0460
Toxicology	0383
Home Economics	0386

PHYSICAL SCIENCES

Pure Sciences

Chemistry	
General	0485
Agricultural	0749
Analytical	0486
Biochemistry	0487
Inorganic	0488
Nuclear	0738
Organic	0490
Pharmaceutical	0491
Physical	0494
Polymer	0495
Radiation	0754
Mathematics	0405
Physics	
General	0605
Acoustics	0986
Astronomy and Astrophysics	0606
Atmospheric Science	0608
Atomic	0748
Electronics and Electricity	0607
Elementary Particles and High Energy	0798
Fluid and Plasma	0759
Molecular	0609
Nuclear	0610
Optics	0752
Radiation	0756
Solid State	0611
Statistics	0463

Applied Sciences

Applied Mechanics	0346
Computer Science	0984

Engineering	
General	0537
Aerospace	0538
Agricultural	0539
Automotive	0540
Biomedical	0541
Chemical	0542
Civil	0543
Electronics and Electrical	0544
Heat and Thermodynamics	0348
Hydraulic	0545
Industrial	0546
Marine	0547
Materials Science	0794
Mechanical	0548
Metallurgy	0743
Mining	0551
Nuclear	0552
Packaging	0549
Petroleum	0765
Sanitary and Municipal	0554
System Science	0790
Geotechnology	0428
Operations Research	0796
Plastics Technology	0795
Textile Technology	0994

PSYCHOLOGY

General	0621
Behavioral	0384
Clinical	0622
Developmental	0620
Experimental	0623
Industrial	0624
Personality	0625
Physiological	0989
Psychobiology	0349
Psychometrics	0632
Social	0451



ABSTRACT

Thermal Performance of a Room with Wall Latent Heat Storage

CHUNYAN LIU

Thermal storage use in buildings is a promising approach for the improvement of energy efficiency. In this study, the feasibility and benefits of utilization of phase change materials (PCMs) in building envelope components for thermal storage were investigated.

The phase change material (PCM) gypsum board used in this study was made by soaking conventional gypsum board in a PCM with phase change range of 16.0°C--20.3°C. Both experimental and theoretical studies were performed to investigate the thermal performance of the PCM gypsum board when used in a passive solar building. The experimental study was conducted in a full scale outdoor test-room with the PCM gypsum board as inside wall lining. The test room was equipped with a computerized data acquisition and control system for transient thermal measurements. An explicit finite difference model was developed to simulate the transient heat transfer process in the walls with PCM gypsum board as inside lining. The model takes into account the transient boundary conditions, absorbed solar radiation, the melting/freezing of the PCM and employed a nonlinear film coefficient. Reasonable agreement between the simulation and the experimental results was observed.

The mathematical model may be used in conjunction with other building thermal analysis software to evaluate the design parameters and the operational characteristics of buildings with wall latent heat storage. This study shows that the utilization of the PCM gypsum board in a passive solar building can effectively limit room overheating by 4-5°C during the daytime and reduce the heating load at night significantly.

ACKNOWLEDGEMENT

The author wishes to express her sincere gratitude to her thesis supervisor, Dr. Andreas K. Athienitis, for his expert guidance and continued support throughout this study.

Special thanks to Dr. D. Hawes, Mrs. D. Banu, research associate and Dr. D. Feldman for their providing the PCM gypsum board, their encouragement and helpful discussion on the project. Many thanks to Dr. R. Zmeureanu and Dr. S. Lin for their helpful consultation. Also thanks are due to Mr. Joseph Zilkha for his technical assistance in the installation of the experimental facilities.

This research was made possible through the support of the Centre for Building Studies (CBS), Concordia University, with its academic, friendly climate and advanced computational facilities.

Finally, my deepest appreciation goes to my parents, my sister and all my friends, for their love, encouragement and support.

TABLE OF CONTENTS

List of Figures	ix
List of Tables	xiii
Nomenclature	xiv

CHAPTER 1 INTRODUCTION

1.1	Energy storage in buildings	1
1.2	Sensible heat storage	4
1.3	Latent heat storage	4
1.4	Advantages of the use of latent heat storage	5
1.5	Phase change materials (PCMs)	6
1.6	Objectives of the thesis	8

CHAPTER 2 LITERATURE REVIEW

2.1	Material development	12
2.2	Development of heat storage devices	13
2.3	PCM gypsum board	14
2.4	Incorporating methods	17

CHAPTER 3 EXPERIMENTAL STUDIES

3.1	Previous studies	19
3.2	Objectives of the experimental study	19
3.3	Experimental facilities	20
3.4	Experimental methodology	25
3.5	Experimental procedure	30
3.6	Analysis of results	32

CHAPTER 4 MATHEMATICAL MODEL

4.1	Introduction	54
4.2	Previous models	54
4.3	Modelling assumptions	56
4.4	Governing equations	59
4.5	Determination of the latent heat flow	61
4.5.1	Previous models	62
4.5.2	The DSC test	64
4.5.3	Simulation of the latent heat flow	69
4.6	Finite difference thermal network model	71
4.7	Numerical experiments and results	75

Chapter 6 CONCLUSION AND RECOMMENDATION FOR FUTURE WORK

5.1	Summary	91
5.3	Recommendations for future work	93

REFERENCES95
-------------------	-----------	------------

APPENDIX A

Data resource for the computer model PCMBOARD	100
---	-----

APPENDIX B

Computer model PCMBOARD	104
-----------------------------------	-----

APPENDIX C

Transient inside film coefficient	106
---	-----

LIST OF FIGURES

No.	Figures	Pages
2.1	The development of a latent heat storage system	11
3.1	Test-room Schematic	21
3.2	Cross-section and floor plan of the test room	22
3.3	A setpoint profile with night setback	26
3.4	Locations of major measuring sensors	28
3.5	Comparison of the thermal response of the PCM and ordinary gypsum boards (cold sunny day-1, air temperature control with hour 17:00 to 6:00 night setback	34
3.6	Comparison of the thermal response of the PCM and ordinary gypsum boards (cold sunny day-2, air temperature control with hour 17:00 to 6:00 night setback	35
3.7	Comparison of the thermal response of the PCM and ordinary gypsum boards (cold sunny day-3, air temperature control with hour 17:00 to 6:00 night setback	36
3.8	Comparison of the thermal response of the PCM and ordinary gypsum boards (cold sunny day-4, air temperature control with hour 17:00 to 6:00 night setback	37

3.9	Comparison of the thermal response of the PCM and ordinary gypsum boards (cold cloudy day, air temperature control with hour 17:00 to 6:00 night setback	39
3.10	Comparison of the thermal response of the PCM and ordinary gypsum boards (mild semi-cloudy day, air temperature control with hour 17:00 to 7:00 night setback	40
3.11	Comparison of the thermal response of the PCM and ordinary gypsum boards (mild semi-cloudy day-1, air temperature control with hour 16:00 to 7:00 night setback	42
3.12	Comparison of the thermal response of the PCM and ordinary gypsum boards (mild semi-cloudy day-2, globe temperature control with hour 16:00 to 7:00 night setback	43
3.13	Comparison of the thermal response of the PCM and ordinary gypsum boards (mild semi-cloudy day-3, globe temperature control with hour 16:00 to 7:00 night setback	44
3.14	Comparison of the thermal response of the PCM and ordinary gypsum boards (mild sunny day, air temperature control with constant setpoint	45
3.15	Comparison of the thermal response of the PCM and ordinary gypsum boards (mild semi-cloudy day, air temperature control with constant setpoint	46
3.16	Thermal performance of the test room with PCM gypsum board applied	48

3.18	Auxiliary heating and room temperature with PCM wallboard installed (mild-sunny day)	52
3.19	Auxiliary heating and room temperature with PCM wallboard installed (mild-cloudy day)	53
4.1	Conceptual temperature distribution across the PCM gypsum board during a freezing process	58
4.2	Schematic heat transfer system for the mathematical model	59
4.3	The DSC test	65
4.4	DSC test results of BS gypsum board (a) with testing rate 2 °C/min, (b) with testing rate 0.15 °C/min	67
4.5	A schematic diagram for the DSC curve	68
4.6	Finite difference procedure, (a) the physical system and nodal arrangement; (b) thermal network model	71
4.7	Comparison between the numerical and the experimental results for a freezing process, front surface temperatures of the PCM and ordinary gypsum boards	76
4.8	Comparison between the mathematical modelling and the experimental results for a melting process, front surface temperatures of the PCM and ordinary gypsum boards	77
4.9	Simulation of the surface temperatures of PCM and ordinary gypsum boards (for a freezing process during a cold sunny day with 23 to 16 °C night setback)	79

4.10	Simulation of the surface temperatures of PCM and ordinary gypsum boards (for a freezing process during a mild cloudy day with 23 to 16 °C night setback)	80
4.11	Simulation of the surface temperatures of PCM and ordinary gypsum boards (for a freezing process during a cold sunny day with 22 to 18 °C night setback)	81
4.12	Simulation of the surface temperatures of PCM and ordinary gypsum boards (for a freezing process during a mild sunny day with 22 to 18 °C night setback)	82
4.13	Simulation of the surface temperatures of PCM and ordinary gypsum boards (for a freezing process during a mild sunny day with constant setpoint)	83
4.14	Simulation of the surface temperatures of PCM and ordinary gypsum boards (for a freezing process during a cold sunny day with constant setpoint)	84
4.15	Simulation of the surface temperatures of PCM and ordinary gypsum boards (for a melting process during a cold sunny day)	85
4.16	Simulation of the surface temperatures of PCM and ordinary gypsum boards (for a melting process during a mild sunny day)	86

LIST OF TABLES

No.	Tables	Pages
1.1	Latent heat and specific heat capacity of some materials	6
2.1	Thermal properties of butyl-stearate (BS) and BS gypsum board	17
3.1	Main building parameters of the test room	23
3.2	Measured parameters during the experimental study	29
3.3	Record of experiments	31
5.1	Heating power saving from the use of 1 m ² BS gypsum board (23 to 16 °C night setback used)	88
5.2	Heating power saving from the use of 1 m ² BS gypsum board (22 to 18 °C night setback used)	89
5.3	Heating power saving from the use of 1 m ² BS gypsum board (constant setpoint 20 °C used)	90
A.1	Nodal parameters for the explicit finite model	103

NOMENCLATURE

C_i	heat capacity of node i , J/K;
C_l	specific heat of a material at liquid state, kJ/kg.K;
C_m	specific heat of a material at mushy state, kJ/kg.K;
C_s	specific heat of a material at solid state; kJ/kg.K;
H	latent heat, J/kg;
L	latent heat value given by a completed freezing or melting process, J/kg;
L_p	latent heat value given by a phase transition occurs in a temperature range of T_1 to T_2 , J/kg;
Q_{es}	average energy saving from unit area of the PCM board, W/m ² ;
Q_s	sensible heat storage, kJ;
R	heating or cooling rate of DSC test, °C/sec;
R_{ij}	thermal resistance between node i and its adjacent node j , K/W;
T	temperature, °C;
T_1, T_2	melting and freezing points, °C;
ΔT	temperature change of a material, °C;
T_{actual}	measured room air or globe temperature, °C;
T_{air}	room air temperature, °C;

T_{iso}	inside surface temperature of ordinary board, °C;
T_{isp}	inside surface temperature of PCM board, °C;
T_o	outside air temperature, °C;
T_{sp}	setpoint of room air or globe temperature, °C;
T^*	scaled temperature;
T_i^p	temperature of node i at time step p, °C;
T_j^p	temperature of an adjacent node to node i, node j, at time step p, °C;
c_p	specific heat of a material, kJ/kg.K;
f_s	solid fraction in the two-phase region at the solidus front;
$f(T)$	temperature dependent heat transfer function;
h_{in}	transient inside film coefficient, W/m ² ·°C;
h_{out}	outside film coefficient, W/m ² ·°C;
h_{so}	inside surface film coefficient for ordinary gypsum board, W/m ² ;
h_{sp}	inside surface film coefficient for PCM gypsum board, W/m ² ;
k	thermal conductivity, W/m·°C;
m	sample mass, kg;
q	latent heat flow, W/m ² ;
q_i^p	latent heat flow released or absorbed by node i at time p, W/m ² ;
q_s	intensity of solar radiation, W/m ² ;
q_s^p	intensity of solar radiation at time step p, W/m ² ;
q_{sp}	the peak value of solar radiation intensity, W/m ² ;

t	time, s;
t_{sr}	sunrise time on the surface, s;
t_{ss}	sunset time from the surface, s;
x	distance from origin of x axis, m;

SUBSCRIPTS

i	the node number in the thermal network model;
j	the node number of an adjacent node to node i in the thermal network model.

SUPERSCRIPT

p	the time step number in the thermal network model.
-----	--

GREEKS

α	surface absorptivity;
ρ	density, kg/m^3 ;
$\Delta\tau$	time step, s.

CHAPTER 1 INTRODUCTION

1.1 ENERGY STORAGE IN BUILDING

Energy consumption in building mechanical systems forms an important part of overall energy consumption, especially in an industrial country. For example, more than 25 quads of energy, which costs \$166 billion, is used for heating, cooling, lighting and ventilation of buildings in the USA every year [1]. Therefore, the improvement of the building energy efficiency deserves a large amount of effort.

There are many approaches to improving the energy efficiency of building mechanical systems, such as more advanced design, more effective HVAC controls, better insulation, new developments in the design of windows and doors, improved methods of ensuring air tightness and vapour sealing as well as more efficient burners, chillers and heat exchangers. However, there is one sphere of activity relating to an alternative energy use, where the scale of development has been markedly less than those in other areas. This field of investigation is the development of appropriate and economical means of thermal energy storage in buildings [2].

An adequate thermal energy storage capacity of a building can be employed to optimize energy efficiencies and, consequently, to suppress the heating and cooling energy costs for the full diversity of space conditioning technologies and strategies. The thermal storage is used for the improvement of building energy efficiency in the following ways [2]:

- a) It makes feasible to use low cost or free energy which would otherwise be wasted because its supply frequently exceeds or is asynchronous with thermal demand. This type of energy may be derived from the following sources:
- 1) passive and/or active solar heating;
 - 2) warm infiltrated air;
 - 3) heat generated by occupants, particularly where large numbers are present as in classrooms, public rooms, theatres and restaurants;
 - 4) heat produced from lighting, cooking, appliances, heat-emitting equipment or exothermic processes [2].
- b) Energy may sometimes be purchased at lower cost during off-peak periods for storage and discharge when full rates would otherwise be charged [2].
- c) In addition to time-shifting of energy consumption, thermal storage can also effect a decrease of the demand peak reflected in less energy costs, smaller equipment sizing and more efficient operation [2].
- d) Excess heat may also be absorbed during the day to moderate the temperature in a building. In this case, the heat is stored for subsequent transfer to cool night air which is circulated over the heat storage surfaces. Thus, using the outside air at night (or whenever the temperature falls to the requisite level) enables a thermal storage system to replace or supplement the function of an air conditioning system [2].
- e) Reduction of furnace cycling and significant improvement of combustion efficiency may be achieved by the use of thermal storage. In this application, the control of the burner is arranged so that the ignition does not occur until the stored heat is depleted, i.e. the

thermostat is set to cause the burner to ignite at a temperature below the freezing point of the phase change material. This arrangement will prolong the furnace's on and off duration. Research has shown that combustion efficiency can be improved between 11% and 54% by reducing short cycle operation. In Canada, it is estimated that the average would be approximately 30% [2].

- f) Higher efficiencies of heat pumps and chillers can be expected where their operating schedules incorporate the longer on and off cycles made possible by the thermal storage [2].

Thermal energy can be stored in three ways:

- 1) as sensible heat;
- 2) as latent heat;
- 3) converted into another form of energy, especially thermo-chemical storage.

Combinations of these techniques may also be used.

1.2 SENSIBLE HEAT STORAGE

Thermal storage as sensible heat is described by:

$$Q_s = \int_{T_1}^{T_2} M.C_p.dT = M.C_p.\Delta T$$

Where,

Q_s = the quantity of stored sensible heat, kJ;

C_p = the specific heat of the material, kJ/kg.°C;

M = the mass of the material, kg;

$\Delta T = T_2 - T_1$, the temperature change of the material.

For a building component, in order to obtain an adequate sensible heat storage capacity, a large temperature swing ΔT or large structure mass are required.

1.3 THERMAL STORAGE AS LATENT HEAT

Latent heat storage is caused by a phase change in a material. The material is called phase change material (PCM). Thermal energy storage may be achieved by melting the PCM and the recovery by freezing it. This phenomenon involves the absorption and the release of a large amount of heat, even though little or no change in temperature occurs. The thermal mechanism of a phase change is as follows: The mean molecular kinetic energy of a substance is higher when it is in liquid state than it is in the solid one. A process of liquid to solid phase transition generates a certain amount of energy which equals the difference between the substance's mean molecular kinetic energy when it is in liquid and solid states. Conversely, the same amount of energy is absorbed by a solid to liquid phase transition process.

1.4 ADVANTAGES OF USE OF LATENT HEAT STORAGE

The utilization of latent heat storage in a comfortable indoor temperature range in buildings can result in an increase of thermal storage capacity in the range of 100%-130% [3]. Compared with the other two forms of heat storage, latent heat storage has the following advantages for building applications (referring to Table 1.1):

- a) It stores large quantities of energy. Table 1.1 shows the values of latent heat and sensible heat of unit mass of some materials;
- b) It avoids the use of large structural mass which is required when sensible heat storage is employed;
- c) Thermal storage may occur in the comfort temperature range;
- d) It stores energy within a small temperature swing and thus avoids the uncomfortable temperature variations which are characteristic of sensible heat storage in buildings;
- e) It avoids seasonal overheating problems which may occur after a succession of hot sunny days and warm nights.

Table 1.1 Latent Heat and Specific Heat of Some Materials

MATERIAL	TRANSITION		SPECIFIC HEAT MJ/m ³ .°C or J/g.K
	TEMPERATURE RANGE °C	LATENT HEAT J/g	
Rocks (granite)	N/A	N/A	2.32
Cement (Portland)	N/A	N/A	1.29
Brick (building)	N/A	N/A	1.58
H ₂ O	0	333	4.18
Na ₂ SO ₄ .10H ₂ O	32.4	254	1.93
CaCl ₂ .6H ₂ O	29.7	171	1.45
Octadecane(99% pure)	27-32	253	1.81
Commercial Wax	35-47	147	1.83
Stearic acid	55-71	191	2.07
Shell paraffin wax 52/54	20-40	45	2.04
Butyl stearate	17-21	140	1.8
Butyl stearate gypsum board	17-21	34	1.26

- 1) Data sources: [4],[5],[9],[14] in the reference list;
- 2) Shaded materials are used for sensible thermal storage, others are use for latent thermal storage.

1.5 PHASE CHANGE MATERIALS (PCMs)

PCMs are employed in building applications to obtain latent heat storage within the comfort temperature range. There are many potential implementations of the PCM technology such as

gypsum wallboard incorporating a PCM, latent heat storage integrated into room heaters or air ducts, preheating the cold side air in heat pumps, curtain walls containing a PCM, water heaters with PCM storage and heat recovery in thermally cyclic processes. The characteristics required for a PCM to be considered suitable for incorporation in building materials or HVAC devices as heat storage means are described below [4]:

a) Thermal properties

Phase transition temperature: 17°C to 36°C, latent heat of fusion: 130-200 J/g;

b) Physical properties

- (1) Phase equilibrium: melting and freezing of all components must be congruent to avoid segregation of material and keep heat exchange within a reasonable temperature range.
- (2)^{*} Vapour pressure: must be in the range to avoid damages of building or HVAC components.
- (3) Density: the higher the density, the greater the amount of heat storage per unit volume, other properties being equal.
- (4) Supercooling: must be avoided because latent heat is not completely released where supercooling occurs. It is a problem with salt hydrates but, fortunately, organic PCMs show little tendency to supercool.
- (5) Chemical stability: because the PCMs are incorporated into building materials, they must have a long service life. •
- (6) Compatibility: PCMs must not react with any material which is likely to be in contact

with them.

- (7) Free from hazard: PCMs must not be toxic nor constitute any hazard in respect to fire, fume or explosion.
- (8) Nuisance free: PCMs can not contain material which emits an odour or causes allergic reactions.
- (9) Good appearance: The PCM must remain within the building material in both solid and liquid states and not cause unacceptable changes in colour or surface condition, e.g. oiliness or crystalline formation [4].

c) Economic factors

The PCMs must be readily available in the market. Their quality must be reliable as per specification. The supply must be abundant and preferably from renewable resources. The net cost must be low. Cost includes processing, containment, maintenance, storage space and heat exchanger requirements. Note that only processing affects the additional cost of its use in building application.

1.6 OBJECTIVES OF THE THESIS

The objectives of this research are as follows:

1. Investigation of the thermal performance of PCM gypsum board used in a passive solar building.
2. Estimation of the benefits from the application of PCM gypsum board in passive solar buildings in terms of the reduction of room overheating and energy savings.

A literature review is summarized in chapter 2 to provide the reader with an overview of the present status of the research work on building latent heat storage issues, including thermal storage materials, the relevant devices used for latent heat storage and the achievements of the incorporation of PCMs with conventional building materials. A previous work (Feldman et. al., 1991) [3] which developed the PCM gypsum board is also introduced.

Chapter 3 presents an experimental study of the thermal performance of the PCM gypsum board and the effects of its application on the overall thermal performance of a passive solar room. The experimental study was conducted in a full scale outdoor test-room with the PCM gypsum board as inside wall lining. The test room was equipped with a computerized data acquisition and control system for the transient thermal measurements. The measurements were performed under various weather conditions. The space temperature was controlled by constant setpoint with or without night setback.

Chapter 4 presents a finite difference thermal network model developed to analyze the transient heat transfer process in the walls with PCM gypsum board as inside lining. The model takes into account the transient boundary conditions, absorbed solar radiation, the melting/freezing of the PCM and employed a nonlinear film coefficient. A computer program, PCMBOARD, was developed to perform the computation. Comparisons between the numerical and experimental results are presented. The estimations of energy saving from the use of PCM gypsum board were given from the simulations for various weather conditions and setpoint temperatures.

Finally, the conclusions on the benefits obtained from the utilization of the PCM gypsum board as a building envelope component are summarized in chapter 5. Extensions of the present work are then recommended.

CHAPTER 2 LITERATURE REVIEW

Research with respect to PCMs for building thermal storage applications can be separated into two categories. One is the development of the suitable phase change materials which possess the required characteristics for building applications. The other is the development of thermal storage devices with high heat exchange efficiency. Figure 2.1 shows a block diagram which provides an overview of the various efforts in the development of a latent heat storage system.

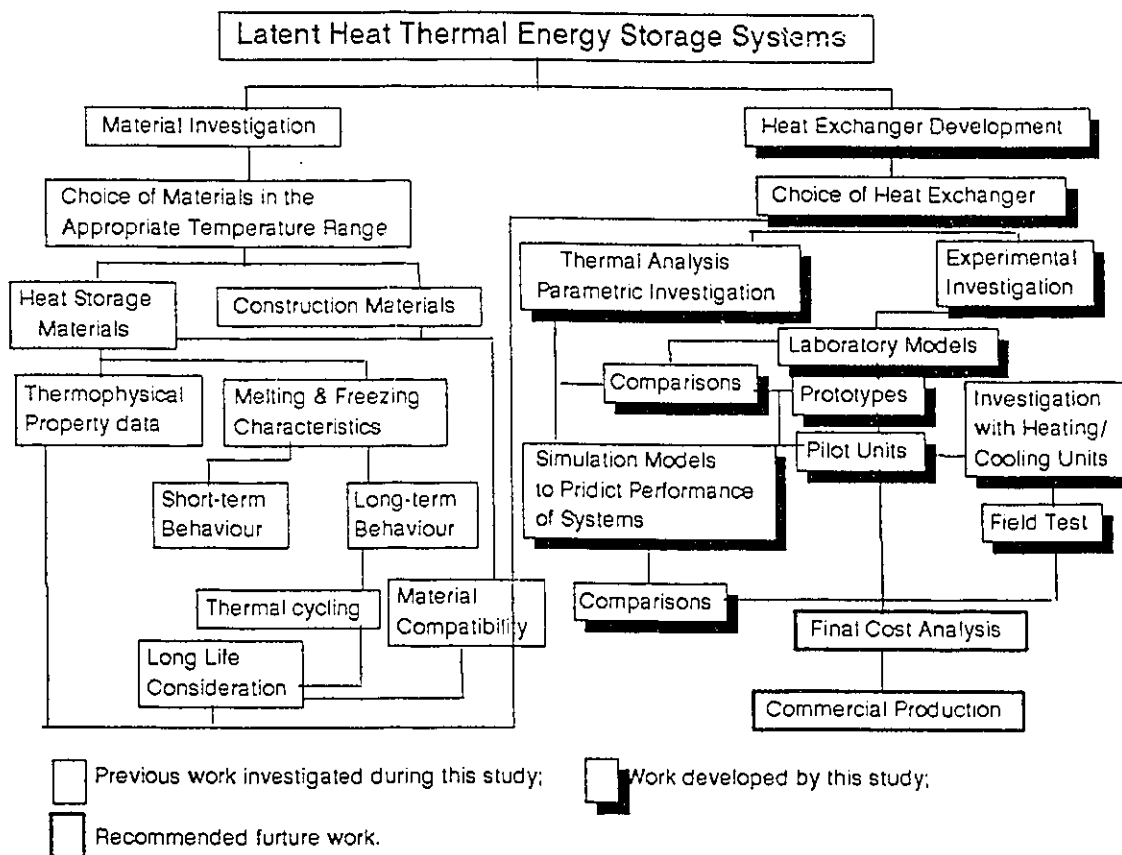


Figure 2.1 The development of a latent heat storage system

2.1 MATERIAL DEVELOPMENT

The utilization of PCMs in the application of building thermal storage has been a subject of considerable interest ever since the first reported application in the 1940s [10]. Later on, facing the pressure of energy crises in all over the world, much work has been done on the development of suitable PCMs which could be used as means of building thermal energy saving. Since the late 1970s, studies have been reported by many authors, such as, Feldman, Shapiro and Fazio (1983, Canada), Abhat (1977, 1981, 1982, FRG), Van Galen (1986, Netherland), Salyer and Sircar (1985, USA), Shibasaki and Fukuda (1985, Japan), Sayigh (1990, Canada) and Hawes, Banu and Feldman (1989, 1990, Canada). In these studies, the PCMs usually considered were of two types, in-organic and organic groups. The in-organic one is mainly comprised of salt hydrates such as Glauber's salt ($\text{Na}_2\text{SO}_4 \cdot 10\text{H}_2\text{O}$) and calcium chloride hexahydrate ($\text{CaCl}_2 \cdot 6\text{H}_2\text{O}$). The organic one includes paraffins such like octadecane, fatty acids and fatty acids esters such like butyl stearate. The problems of supercooling and phase separation existed in the salt hydrates have been overcome to a large extent and some commercial products are available. The organic group of PCMs is thermally more stable but has lower volumetric heat of fusion and is more expensive than the in-organic one. However, they are easier to be encapsulated and immersed into ordinary building materials. Research has proved that both these two classes of PCMs can be used in building thermal storage applications. They may be employed in different thermal storage systems according to their characteristics.

2.2 DEVELOPMENT OF HEAT STORAGE DEVICES

Studies focused on the improvement of active solar system efficiency were largely reported since 1970's. San Tamouris and Lefas (1988, Greece) designed a new heat exchanger based on the rolling cylinder principle. Yanadori (1989), Hirata and Ueda (1988, Japan), and Sakitani and Honda (1989, Japan) contributed their work on the development of different PCM containers and the improvement of heat transfer conditions. Hirose and Saitah (1990, Japan) developed a unique latent heat thermal energy storage/heat pump system using spherical capsules, a heat pump was introduced to resolve the supercooling problem of many salt hydrates systems.

Contributions on the improvement of passive solar system thermal efficiency made it more feasible to apply the PCMs in building applications. A significant accomplishment was to introduce PCM, with phase change point in the human comfort temperature range, into ordinary building material, such as gypsum board and concrete. Neeper (1989) discussed the benefits of distributed PCM thermal storage in passive solar buildings. Salyer (1989) and Kedl (1989) performed theoretical and experimental studies concerning the thermal performance of PCM gypsum board. Peippo, Kauranen and Lund (1991) presented a computational method for the determination of the optimum phase change temperature and thickness of a PCM wallboard. However, not much has been reported on the theoretical and experimental studies of the thermal performance of PCM wallboard used in an actual building.

The optimization of the latent thermal storage system is dependent on the energy collection and

delivery characteristics of the system [12]. In the applications of active solar systems and heat pumps, PCMs have high phase change point (higher than normal human comfort temperature). Latent heat has to be transferred by heat exchanger between the solar collector and normal comfort temperature zone. In passive solar systems, the PCMs are incorporated into conventional building components, such as gypsum board and concrete. Their phase transitions take place in a normal comfort temperature range, from 16°C to 30°. The generated and absorbed latent heat is transferred directly between building components and the space and no extra heat exchange systems are required. Passive solar systems are more promising because of their simplicity of concept and they avoid heat transfer problems of active solar ones. PCM gypsum board is one of the most promising thermal storage options.

2.3 PCM GYPSUM BOARD

PCM gypsum board is made by the incorporation of PCM into ordinary gypsum board. The incorporated PCM absorbs and releases latent heat during its phase transition. The gypsum matrix acts as a vehicle to contain the PCM and transfer the released or absorbed heat to or from the space. The PCM gypsum board is unique because it can be used as a conventional building component and a latent heat storage device as well.

A major advance in the development of PCM gypsum board was reported by Feldman et al. (1990) [3]. In this work, the chosen PCM was an organic material, Butyl Stearate (BS). BS possesses the thermodynamic and kinetic characteristics for the low temperature heat storage

mentioned in Chapter 1. It has relatively low phase change point and a high latent heat of transition per unit mass. It exhibits a small volume change during the phase transition and does not supercool during its freezing. It possesses good chemical stability, low vapour pressure at room temperature, high flash point and high auto-ignition temperature; Moreover, it is non-toxic, non-corrosive and odourless [3].

BS is a commercial product (Emery 2325) and consists of a mixture of 49% butyl stearate and 48% butyl palmitate. It represents more than half of the stearic acid esters production. The fatty acid esters are already produced in large amounts for plastic, cosmetic, textile and lubricant industries and many of them are obtained from renewable sources such as oil seeds and tallow [3].

Gypsum wallboard was chosen as an appropriate vehicle for the PCM (BS), because it is a common building product which is easily adapted to energy storing applications. It can also be produced and marketed by existing manufacturing and sales facilities. The other results of this work were summarized as follows [3]:

The flexural strength of laboratory produced thermal storage wallboard compared well with values obtained for conventional wallboard [3].

Durability of the samples and components of thermal storage wallboard was evaluated by the use of accelerated freeze-thaw tests. The results obtained were satisfactory [3].

Compatibility tests with representative paints (ester- and alkyd-based) showed no sign of any peeling, blistering, or evidence of exudation of the BS one year after manufacture [3].

The water absorption test demonstrate that this product absorbs less than 1/3 as much water as plain wallboard and is, therefore, a potential candidate for use in humid environments [3].

For a rise of about 4°C through the melting range of PCM, 1 m² of energy storing wallboard, with 22% BS, has a total thermal storage capacity of 370 kJ. This capacity was computed by adding the sensible heat capacity of gypsum alone (33 kJ) with the sensible heat capacity of BS (16 kJ) and the latent heat capacity of BS (321 kJ) [3].

The BS gypsum board developed for this work contains about 25% by weight proportion of butyl stearate. The thermal properties of this PCM gypsum board were tested by using the differential scanning calorimeter (DSC). Table 2.1 presents some physical and thermal properties of the butyl stearate and the BS gypsum board .

Table 2.1 Thermal properties of butyl-stearate and BS gypsum board

Material	Density kg/m ³	Specific heat kJ/kg.°C	Thermal conductivity W/m.°C	Phase change range °C	Latent heat J/g
Butyl stearate	855 ⁽⁴⁾	1.80 ⁽⁷⁾	0.20 ⁽⁴⁾	17.8~23 ⁽²⁾	140 ⁽²⁾
Gypsum board	720 ⁽⁷⁾	1.08 ⁽⁷⁾	0.187 ⁽⁷⁾	N/A	N/A
BS gypsum board	900 ⁽⁷⁾	1.26 ⁽⁷⁾	0.214 ⁽⁴⁾	16.5~20.9 ^(*)	30.7 ^(*)

Note: 1) numbers in brackets refer to data sources and are consistent with the ones in the references list;

2) * denotes the DSC test result from the Building Materials Laboratory at the CBS, Concordia University.

2.4 INCORPORATING METHODS

The incorporation of PCM into gypsum wallboard has been a subject of research in recent years.

Methods of incorporation are [3]:

- incorporation by capsules, comprising the addition of small self-contained capsules of PCM when blending the components of the building material;
- direct incorporation, incorporating the PCM with other components which make up the building material;
- immersion, incorporating PCM by direct immersion of regular wallboard at room temperature into a container of PCM at 80 °C.

The first two methods are suitable for industrial manufacturing. The direct incorporation and the immersion methods were discussed and used in previous works by Shapiro et al. (1987) and Feldman et al. (1990) [3]. The immersion method can be conveniently used for experiments. This method was also used by Feldman, Shapiro, Fazio, Hawes and Banu (1986) for their studies of energy storing wallboard [5].

To summarize the literature review, the passive solar systems are more promising because of their simplicity of concept and they avoid heat transfer problems found in active solar ones. Recent research shows that, as an application for passive solar thermal storage, the PCM gypsum board and concrete have great potential in terms of the improvement of building energy efficiency. The feasibility and benefits of the utilization of BS gypsum wallboard deserve intensive studies.

CHAPTER 3 EXPERIMENTAL STUDIES

3.1 PREVIOUS STUDIES

Most of the existing studies concerning the use of PCMs for building application focused on the development of suitable materials on a laboratory scale. With respect to the thermal performance of PCM gypsum board applied in a passive solar room, theoretical studies have been carried out by Peippo et al. (1991) [12] and Kedi (1991) [13]. Kedi (1991) [13] performed an experiment investigating the thermal performance of PCM gypsum board in the laboratory. During his experiment, the two surface temperatures (front and back) of the PCM gypsum board were controlled at certain constant values by two heating and/or cooling panels; therefore the results from his study could not be applied to actual passive solar buildings. However, this work developed valuable knowledge concerning the thermal properties of PCM gypsum board and the test methodology. Whether the PCM in gypsum wallboard applied to a passive solar room as inside lining is able to undergo its solid-liquid phase transition and how the application affects the overall building performance are not known yet and a full-scale experimental study is needed.

3.2 OBJECTIVES OF THE EXPERIMENTAL STUDY

The objectives of this experimental study are:

- 1) To investigate the thermal performance of the PCM gypsum board applied in a full-scale passive solar room;

- 2) To test the effect of the use of PCM gypsum board on the overall thermal performance of an actual passive solar room in the following aspects:
 - a) reduction of overheating;
 - b) storage of extra heat and its reuse;

3.3 EXPERIMENTAL FACILITIES

Test Room

An existing out-door test room, exposed to natural weather conditions, was used for this experimental study. The test room, with its schematic shown in Figure 3.1 and detail structure shown in Figure 3.2, is of light weight construction. It is located in Montreal (45 ° latitude) and has a large double-glazed window facing 10 degrees east of south.

Table 3.1 provides the thermal properties of the test room.

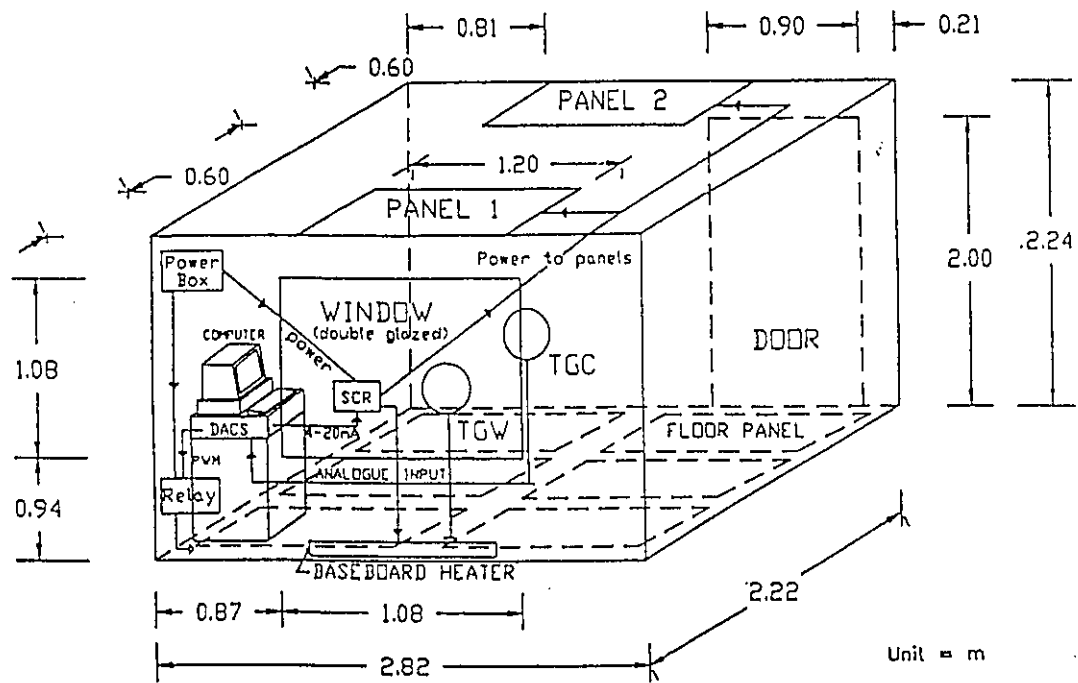


Figure 3.1 Test-room Schematic (from reference [16])

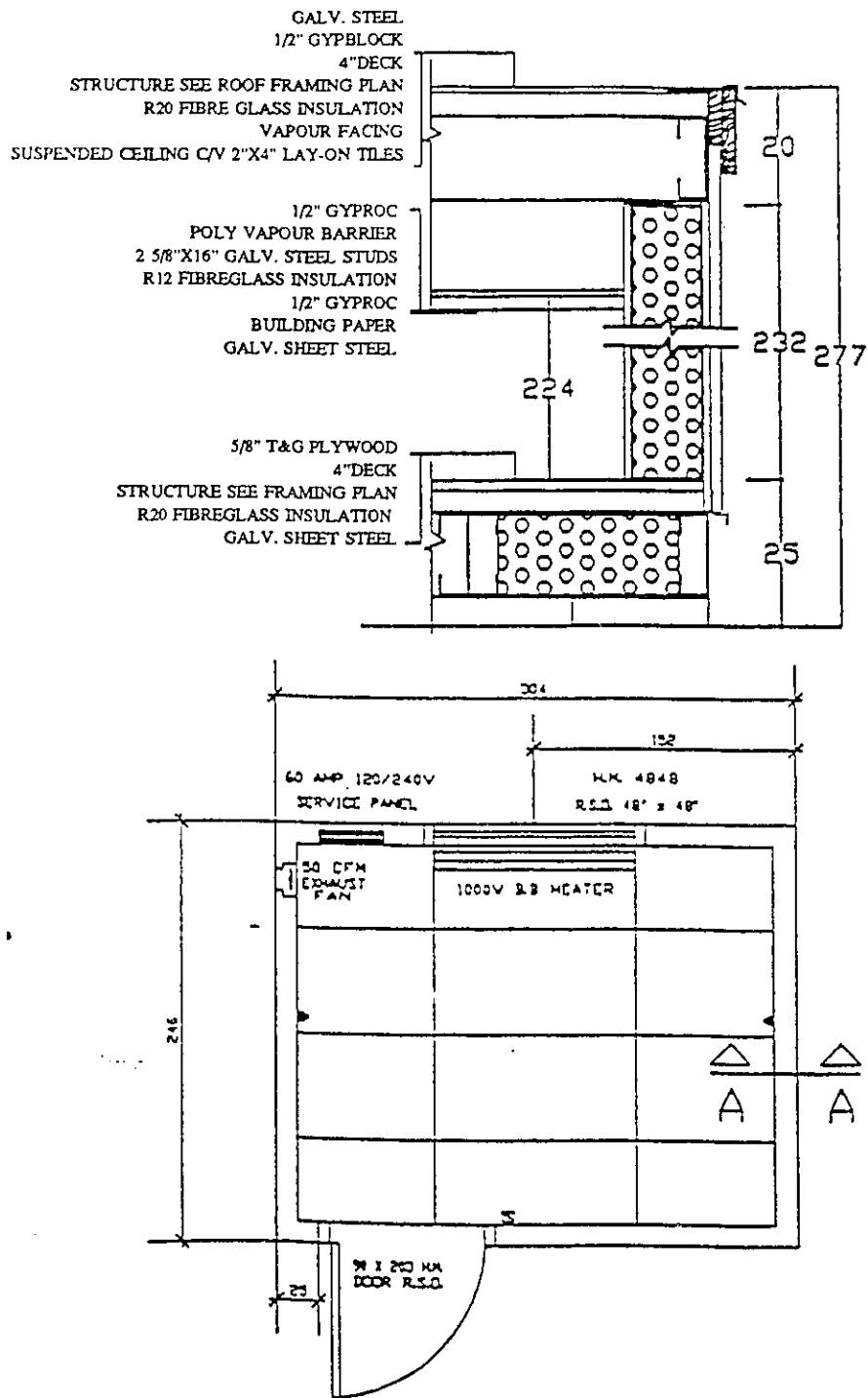


Figure 3.2 Cross-section and floor plan of test-room

Table 3.1 Main parameters of the test-room

Floor area, m ²	7.3
Wall area, m ²	26.8
South-facing glazing, m ²	1.2
Total glazing, including door glazing, m ²	1.7
Door area, m ²	1.8
U-value for walls (without PCM gypsum board), W/m ² °C	0.40
U-value for roof, W/m ² °C	0.24
U-value for floor, W/m ² °C	0.24
U-value for windows, W/m ² °C	3.35
PCM wallboard area, m ²	20
Heating load, W	*1300

* The calculations were based on: inside design temperature, 20 °C, outside design temperature, -26 °C for Montreal.

PCM gypsum board

PCM (BS) gypsum board was made at the Building Materials Laboratory in the Centre for Building Studies according to the "direct immersion" method described in Chapter 2. Ordinary gypsum board of around 20 m² was immersed into liquid butyl stearate at 70 °C for about 100 seconds. The total weight of butyl stearate absorbed was 45 kg and it constitutes 24.8 wt% of the BS gypsum board. The BS gypsum boards possess physical and thermal properties described in Chapter-2 and were installed in the test-room as inside wall lining.

Heating system

The test room was heated by an electric floor heating panel system with 30 °C maximum

allowable floor surface temperature and 1300 W total heating capacity and covers the overall room floor.

Computer aided thermal control system

A computerized data acquisition and control system was employed for the heating system control to maintain the test room air temperature at the required setpoint. The measured data were the room air temperature, outside temperature, room surface temperatures and the intensity of solar radiation. The thermal response of the test room was monitored through these measurements. The controlled parameter, as the output from the control system, was the electric power to the floor radiant heating panels. The room air temperature or a globe temperature sensor was used for the thermostatic control. The control algorithm computed the desired output power level based on the proportional control relationship (Athienitis, 1991, [17]):

$$q(t) = K_p (T_{\text{actual}}(t) - T_{\text{sp}}(t))$$

where,

$T_{\text{actual}}(t)$ = measured room air or globe temperature, °C, at time t;

$T_{\text{sp}}(t)$ = setpoint room air or globe temperature at time t, °C.

t = time, second.

The setpoint temperature was programmable as a function of time. The setpoint temperature profiles were selected based on thermal comfort requirements and energy saving considerations. Data acquisition and control were performed by a general purpose computer software package

"Gen-200" [30]. The software contained features which made it an appropriate choice for the present research which required continuous measurement, data storage and computer control. The main advantages of this software were that it was fully menu driven, supported multi-task measurements and controls, allowed real-time modifications of system setup parameters, such as programmable setpoint profile and simplified the operation of the system.

3.4 EXPERIMENTAL METHODOLOGY

The experiment was performed mainly from the end of February to the end of April, 1992. During the experiment, the outside temperature was in a range of $-25\text{ }^{\circ}\text{C}$ to $3\text{ }^{\circ}\text{C}$ and the weather conditions comprised cold sunny days, mild sunny days, cold cloudy days and mild cloudy days. The room air temperature was controlled according to a series of setpoint profiles with or without night setback. For example, when the room temperature is controlled according to a setpoint profile with night setback, shown in Figure 3.3, the air temperature is maintained at $23\text{ }^{\circ}\text{C}$ during the building occupied period (from hour 6:00 to 17:00), and it is set back to $16\text{ }^{\circ}\text{C}$ when the building is unoccupied. When the room air temperature changes, according to the above temperature setpoint profile, the PCM in gypsum board undergoes some solid-liquid transitions in the phase change range of BS, $16\text{ }^{\circ}\text{C}$ to $20.8\text{ }^{\circ}\text{C}$. If the PCM gypsum board undergoes a temperature rise through this range, the PCM will melt and latent heat will be absorbed. On the other hand, if the PCM gypsum board undergoes a temperature drop, the PCM will freeze and the latent heat will be released. When the room temperature is controlled by a constant setpoint without night setback, $20\text{ }^{\circ}\text{C}$, for example, the PCM in the gypsum board can also undergo its

phase transition and perform its thermal storage function. This is because the room temperature often increases beyond 22 °C due to solar gain, and it drops back to 20 °C after sunset.

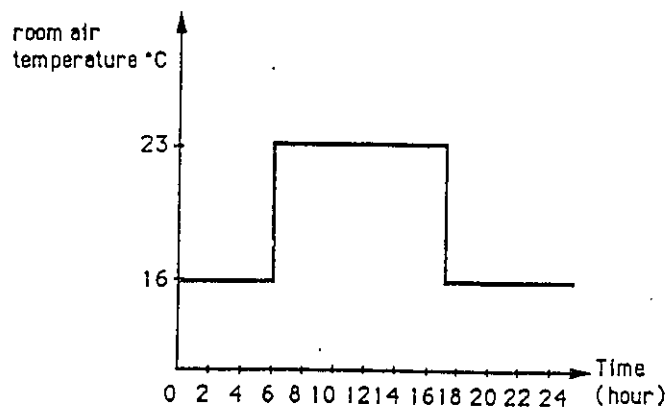


Figure 3.3 A setpoint profile with night setback

To monitor the thermal response of the room with latent thermal storage wallboard, temperatures at approximately 30 different locations in the test room were measured and recorded against actual time. These included the front and back surface temperatures of the PCM wallboard on each wall, the air temperature, the temperature of heating panels, etc. A one square foot piece of the PCM gypsum board was cut from the north wall PCM gypsum board where solar incidence might be obtained and replaced by a piece of ordinary gypsum board. The front and back surface temperatures of this piece of ordinary board were measured and recorded. The same measurements were taken on the PCM gypsum board immediately adjacent to this piece of

ordinary gypsum board. The synchronous measurement showed the different thermal response of these two kinds of gypsum boards under the same ambient conditions. Thermal analysis was then performed from the temperature records at different test room locations. Figure 3.4 shows the locations of major measuring sensors in the test-room. The measured items are listed in Table 3.2.

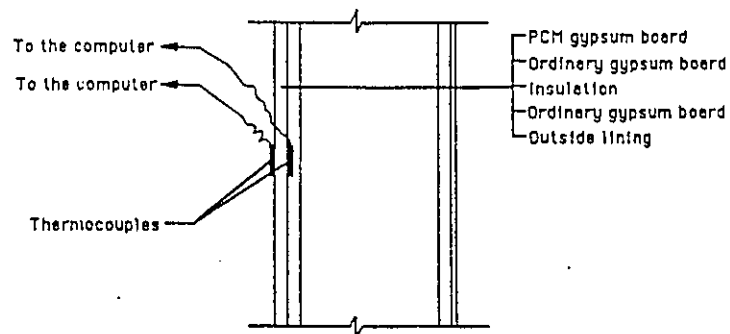
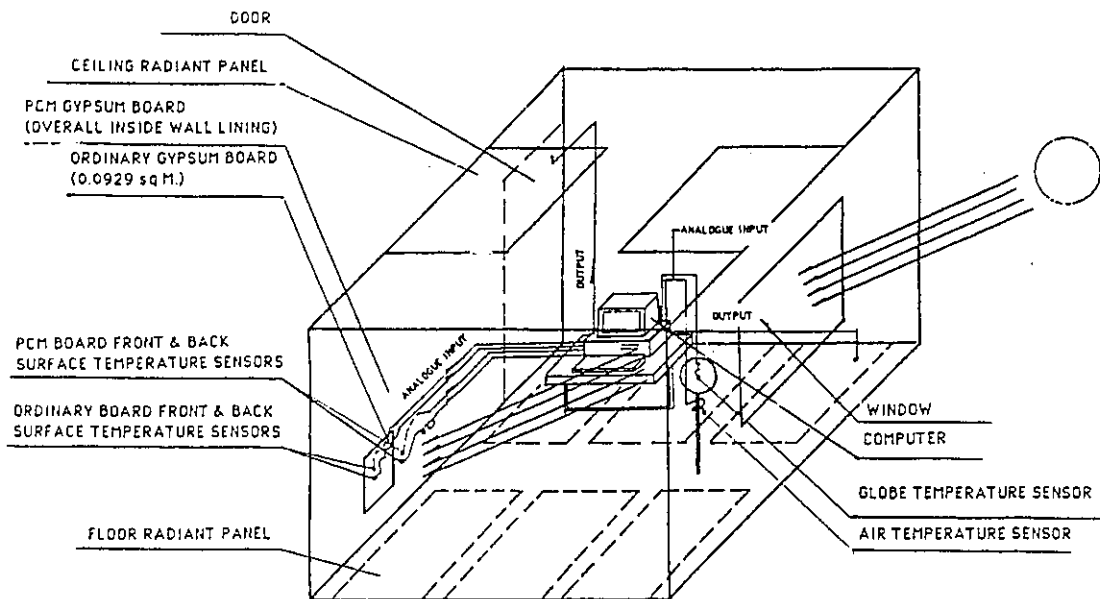


Figure 3.4 Locations of major measuring sensors

Table 3.2 Measured Parameters

Number	Parameters
1	room air temperature at the room centre
2	globe temperature at the room centre
3	globe temperature beside the window
4	front surface temperature of the north wall PCM gypsum board
5	back surface temperature of the north wall PCM gypsum board
6	front surface temperature of the north wall ordinary gypsum board
7	back surface temperature of the north wall ordinary gypsum board
8	front surface temperature of the south wall PCM gypsum board
9	back surface temperature of the south wall PCM gypsum board
10	front surface temperature of the south wall ordinary gypsum board
11	back surface temperature of the south wall ordinary gypsum board
12	interior surface temperature of the ceiling
13	interior surface temperature of the floor
14	front surface temperature of the west wall PCM gypsum board
15	front surface temperature of the east wall PCM gypsum board
16	top surface temperature of the floor heating panel
17	bottom surface temperature of the floor heating panel
18	floor surface temperature
19	room air temperature located 10 cm from the ceiling
20	room air temperature located 15 cm above the floor
21	interior surface temperature of the door
22	solar radiation transmitted through the window
23	solar radiation outside the test room
24	outside air temperature

3.5 EXPERIMENTAL PROCEDURE

1. Set up of the data acquisition and control system including the connections of the measuring sensors and the input channels, the output channel and the heating power;
2. Set up of the control system by creating a computer file required by the software package "Gen-200". The task included defining of the input channels, the scanning items, the saving items, data saving rate, output type (analogue or digital), the output channel and the programming of setpoint profiles, etc;
3. Monitoring of the thermal response of the test room by starting the data acquisition system. The room temperature was controlled at required setpoint;
4. Repeat of the experiment for different weather conditions accompanied with various programmed setpoint profiles. These experiments are summarized in Table 3.3.

Table 3.3 Record of Experiments

No.	Date	sky condition	outside temperature°C	control sensor	high setpoint °C	low setpoint °C	high setpoint period
1	Feb29,92	sunny	-22	air temp.	23	16	6:00-17:00
2	Mar1,92	cloudy	-15	air temp.	23	16	6:00-17:00
3	Mar5,92	sunny	-16	air temp.	23	16	6:00-17:00
4	Mar7,92	cloudy	-18	air temp.	23	16	6:00-17:00
5	Mar9,92	cloudy	-15	air temp.	23	16	6:00-17:00
6	Mar13,92	sunny	-16	air temp.	23	16	6:00-17:00
7	Mar14,92	sunny	-15	air temp.	23	16	6:00-17:00
8	Mar15,92	sunny	-15	air temp.	23	16	6:00-17:00
9	Mar24,92	semi-cloudy	-7	air temp.	23	16	7:00-16:00
10	Apr4,92	sunny	-1	globe temp.	23	16	7:00-16:00
11	Apr8,92	semi-cloudy	0	globe temp.	23	16	7:00-16:00
12	Mar20,93	sunny	-7	air temp.	constant 18	constant 18	N/A
13	Mar21,93	cloudy	-2	air temp.	constant 18	constant 18	N/A
14	Mar22,93	sunny	-2	air temp.	constant 18	constant 18	N/A
15	Mar23,93	sunny	-5	air temp.	constant 18	constant 18	N/A

3.6 ANALYSIS OF RESULTS

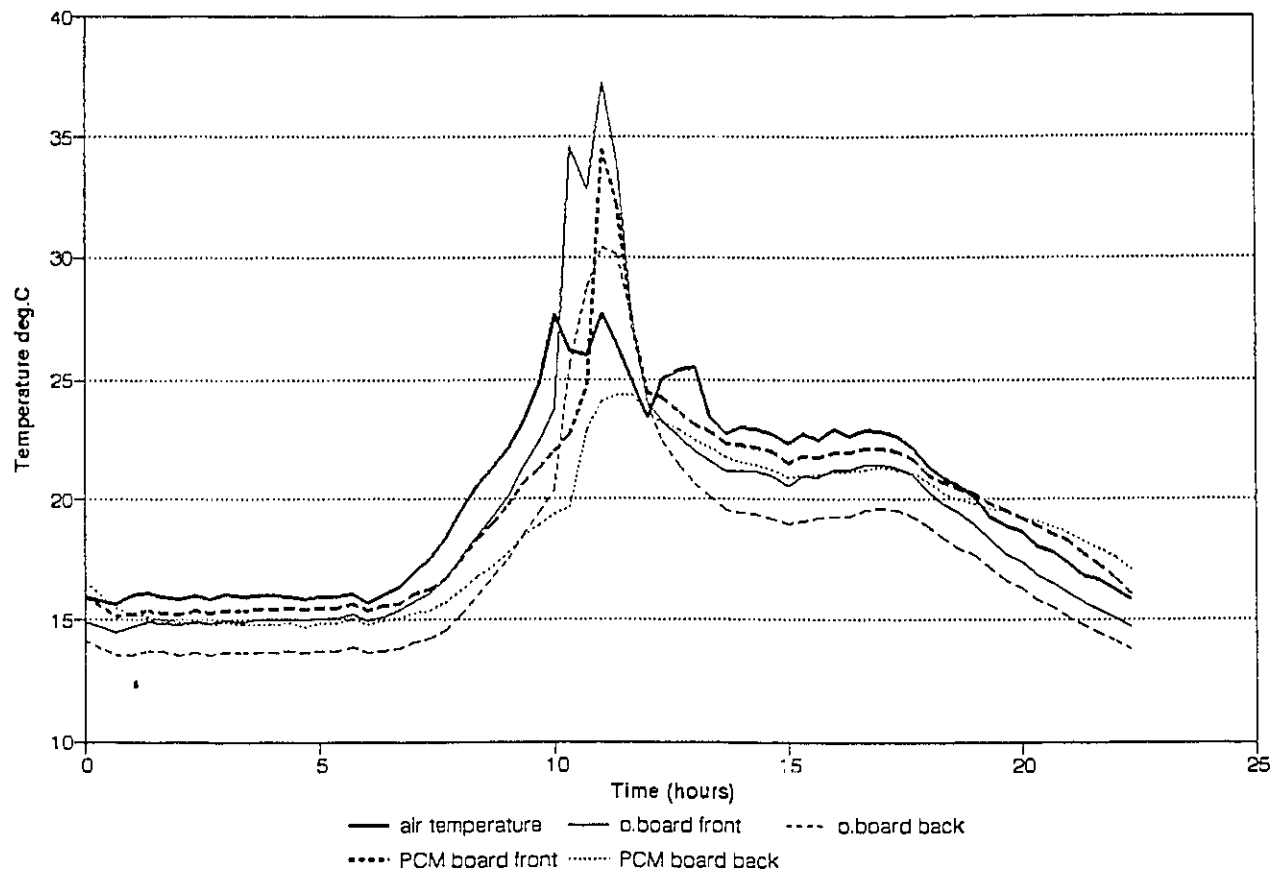
Thermal response of the PCM gypsum board

The thermal response of the PCM gypsum board was investigated by analyzing the experimental results obtained from various test conditions (weather conditions and space setpoint):

The thermal performance of the PCM and the ordinary gypsum boards during cold sunny days are presented in Figures 3.5 to 3.8. In Figure 3.5, "PCM Board Front" and "PCM Board Back" denote the front and back PCM board surface temperature, respectively. "O.Board Front" and "O.Board Back" denote the front and back ordinary board surface temperature, respectively (the same legends are used in other figures presenting the experimental results). Comparison between the surface temperature of the PCM and the ordinary gypsum boards indicates that the temperature rise of the PCM gypsum board was effectively restricted when large amounts of solar gains were presented. The largest front surface temperature difference between the PCM and the ordinary boards was approximately 11 °C at 10:00. The lowered surface temperature of the PCM gypsum board was caused by the heat absorption due to the PCM's melting process. The figure shows that this process started from the front surface at about 7:30 and finished at the back surface at about 10:00. The overall melting period for the full thickness of the PCM gypsum board was two and an half hours. The melting period varies due to the different amount of solar gains and outside temperature. The melting periods obtained from other experiments, shown in Figures 3.6 and 3.7, are two (9:00 to 11:00) and four (7:00 to 11:00) hours, respectively. During these melting processes, the surface temperature of the PCM gypsum board was generally lower

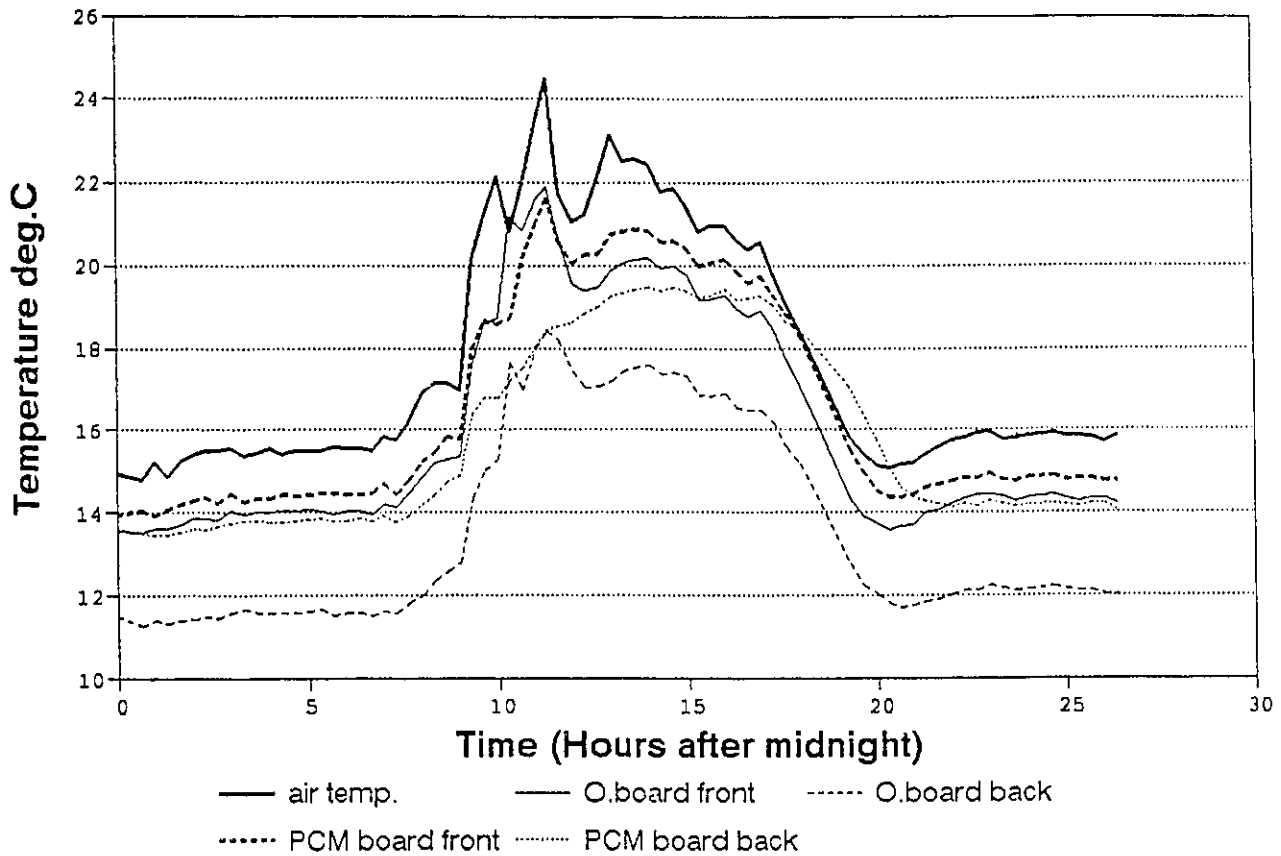
than the ordinary one's two to six °C. It even sometimes remained steady when the air temperature and the ordinary wallboard surface temperature increased largely. Figure 3.8, a result obtained from another cold sunny day, shows that the front surface temperature of the PCM gypsum board maintained steady at around 21 °C, while the ordinary one's increased up to 27 °C.

When the space temperature drops due to the sunset and the setback of the setpoint, the temperature drop of the PCM gypsum board is slower than the ordinary one's. This is because the freezing process occurs and the released latent heat restricts the temperature drop of the PCM gypsum board. Figure 3.6 - 3.8 show a general trend that, during the freezing process, the front surface temperature of the PCM gypsum board was higher than the ordinary one's 1.5 to 2.9 °C (the maximum values). The surface temperature of the PCM gypsum board was even maintained equal to, or higher than the air temperature during the PCM 's freezing process. For example, it was equal to the air temperature for two hours from 17:30 to 19:30 in Figure 3.6. It was higher than the air temperature about 0.2 to 1 °C for three hours (17:30 to 20:30) and two hours (18:00 to 20:00) in Figure 3.7 and 3.8, respectively.



Experimental result for March 5, 92, a cold sunny day with transmitted solar radiation 668 W/M^2 at noon, Control strategy :air temperature control, $K_p=1000 \text{ W/C}$, Low setpoint = 16°C , high setpoint = 23°C , high setpoint from 6:00 to 17:00.

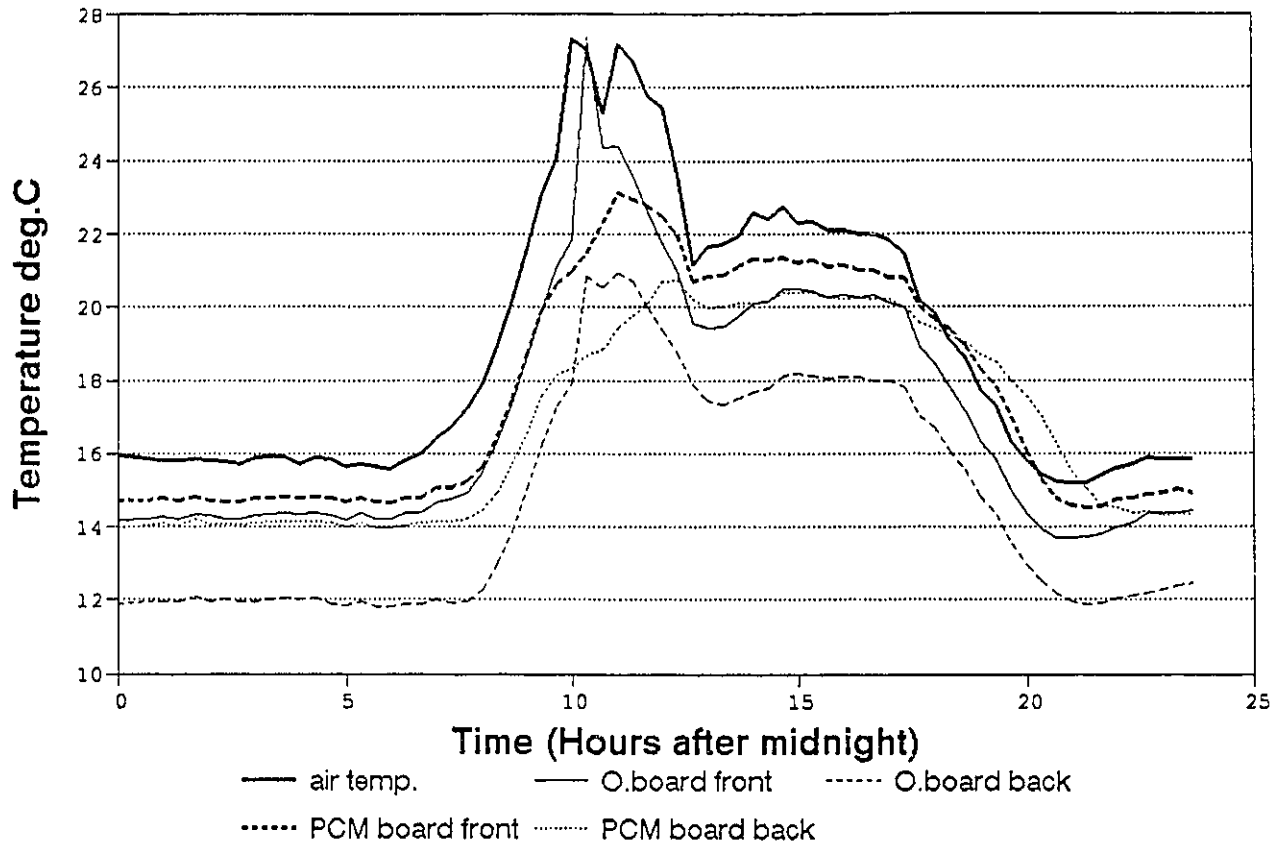
Figure 3.5 Comparison of the thermal response of the PCM and the ordinary gypsum boards (cold sunny day-1, air temperature control with hour 17:00 to 6:00 night setback)



Experimental result for March 13, 1992, a cold sunny day with lowest outside temperature -16°C and transmitted solar radiation 518 W/C at noon.

Control strategy: air temperature control, $K_p = 1000\text{ W/C}$, Low setpoint = 16°C , high setpoint = 23°C high setpoint from hour 6:00 to 17:00.

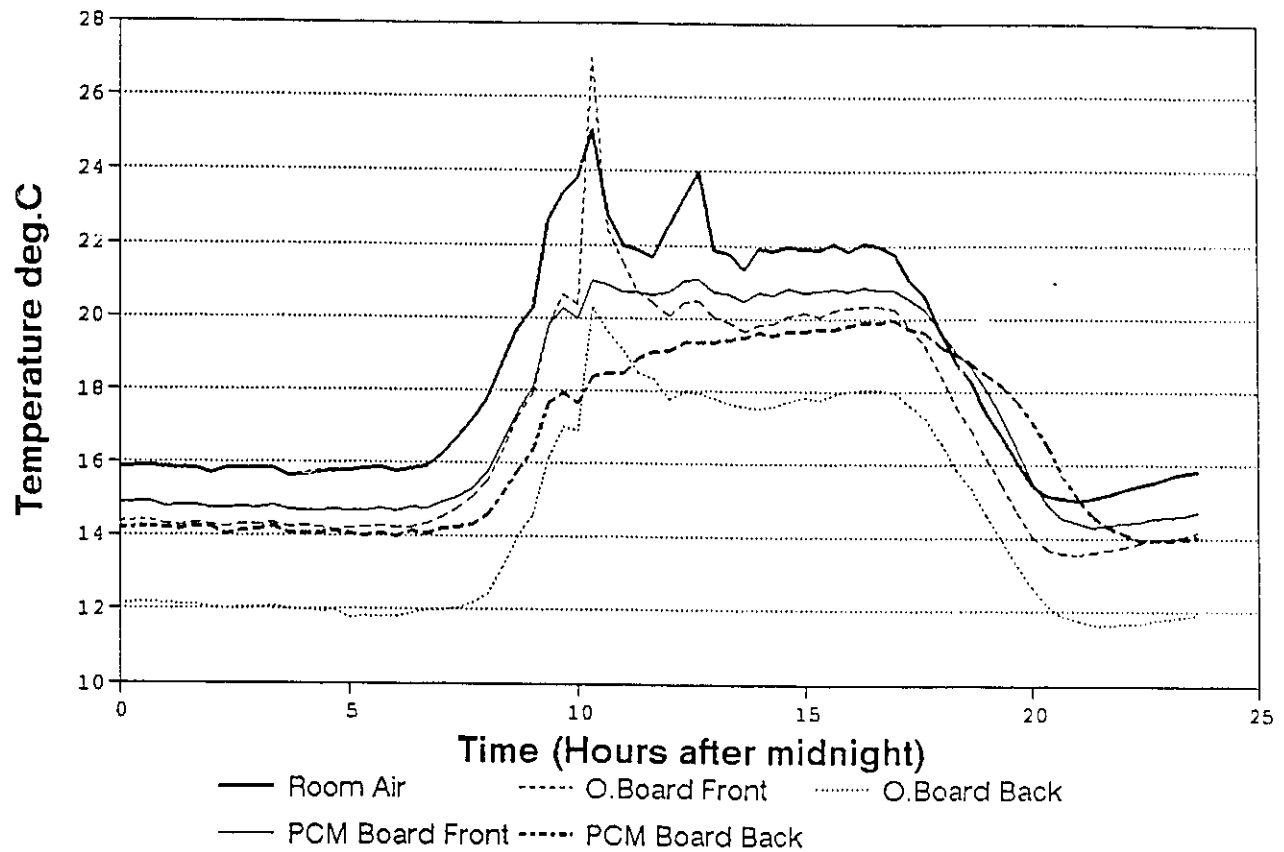
Figure 3.6 Comparison of the thermal response of the PCM and the ordinary gypsum boards (cold sunny day-2, air temperature control with hour 17:00 to 6:00 night setback)



Experimental result on March 15, 1992, a cold sunny day with lowest outside temperature -15°C and transmitted solar radiation 600 W/M^2 .

Control strategy: air temperature control, $K_p = 1000 \text{ W/C}$, Low setpoint = 16°C , high stpoint = 23°C , high setpoint from hour 6:00 to 17:00.

Figure 3.7 Comparison of the thermal response of the PCM and the ordinary gypsum boards (cold sunny day-3, air temperature control with hour 17:00 to 6:00 night setback)



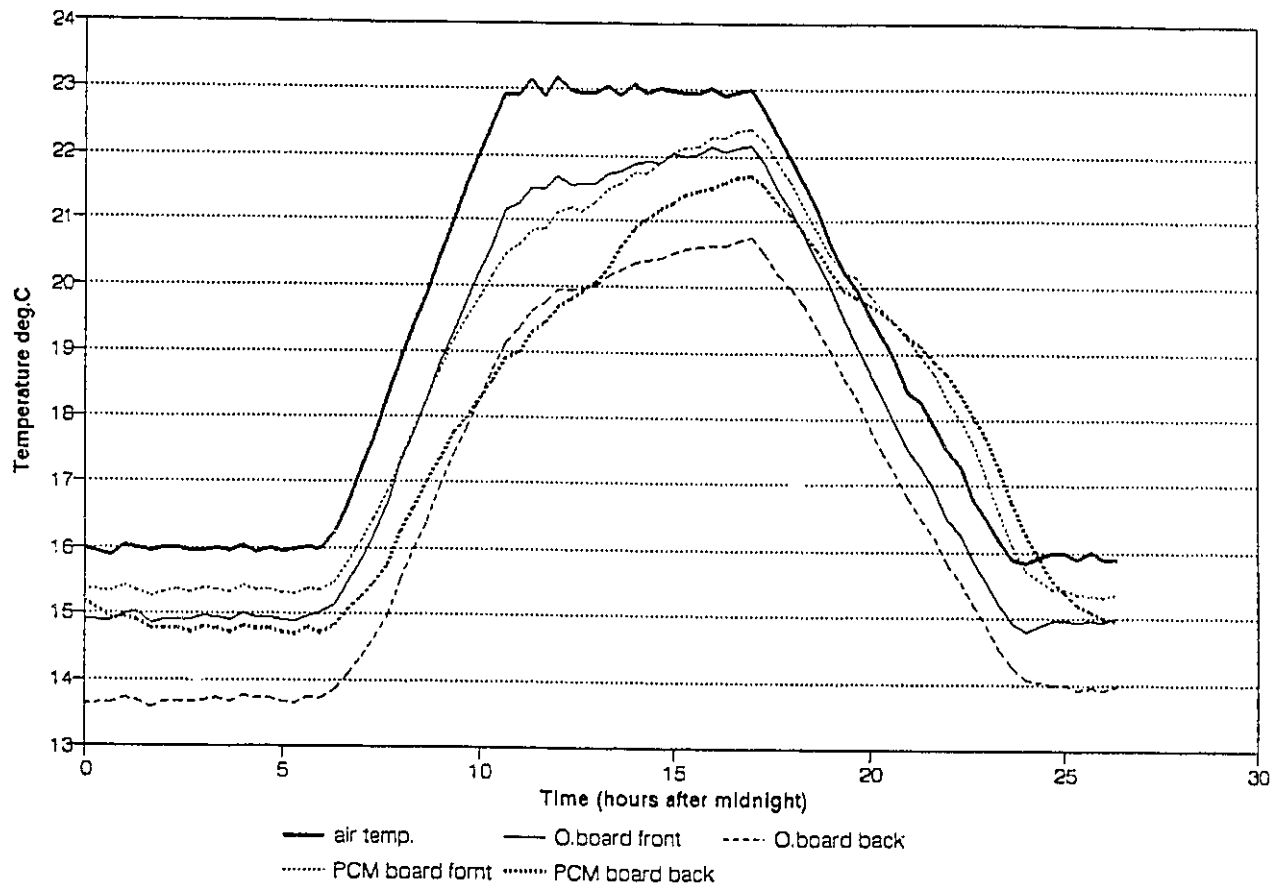
Experimental result on March 14th, 92, a cold sunny day with lowest outside temperature -15°C and transmitted solar radiation 600 W/C at noon.

Control strategy: air temperature control, $K_p = 1000$ W/C, step setpoint from 16°C to 23°C, night setback from 17:00 to 6:00

Figure 3.8 Comparison of the thermal response of the PCM and the ordinary gypsum boards (cold sunny day-4, air temperature control with hour 17:00 to 6:00 night setback)

For a cold cloudy day, the melting period is longer than it is in a sunny day, for example, in Figure 3.9, it was five hours (7:30 to 12:30). During cloudy days, because of the absence of the solar radiation, during melting, the PCM absorbs and stores thermal energy obtained from the auxiliary heating when the space setpoint is changed from 16 °C to 23 °C in the morning. During the evening, when the setpoint is set back from 23 °C to 16 °C, the stored heat is generally released to the space and the front surface temperature of the PCM gypsum board was higher than the room air temperature for maximum of one degree for four hours (20:00 to 24:00). In this case, the application of the PCM gypsum board does not contribute to the heating energy saving or consumption, because the heat absorbed by the PCM's melting is supplied by the auxiliary heating and given back to the space. Obviously, certain amount of energy is lost during this energy charge and release process. But the amount is estimated to be low because the PCM gypsum board is installed as inside wall lining and most released energy is given to the space. The detailed study with respect to energy loss due to the use of PCM gypsum board in cloudy days is not covered by the present work.

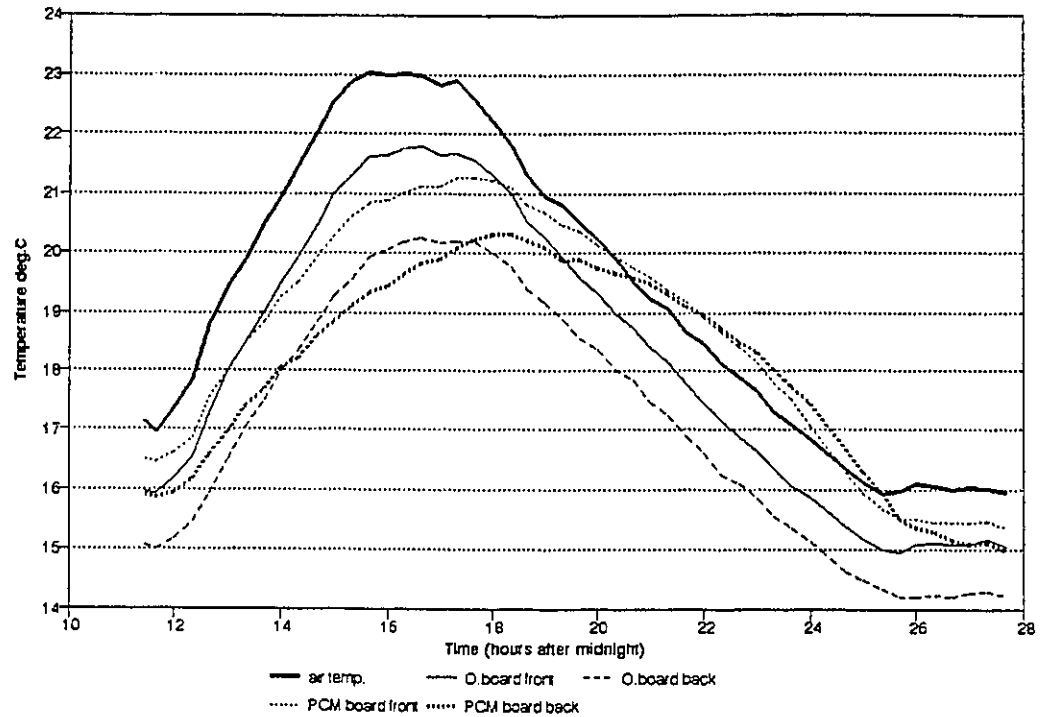
The results obtained from the mild days are similar to the ones obtained from cold days, but with longer freezing process. Figure 3.10 shows that the freezing process lasted nine hours, from 18:00 in the evening until 3:00 in the next morning. The released latent heat kept the front surface temperature of the PCM board higher than the air temperature for 4.3 hours.



Experimental result for March 7, 92, a cold cloudy day .

Control strategy: air temperature control, $K_p = 1000 \text{ W/C}$, Low setpoint = 16°C , high setpoint 23°C , high setpoint from hour 6:00 to 17:00.

Figure 3.9 Comparison of the thermal response of the PCM and the ordinary gypsum boards (cold cloudy day, air temperature control with hour 17:00 to 6:00 night set back)

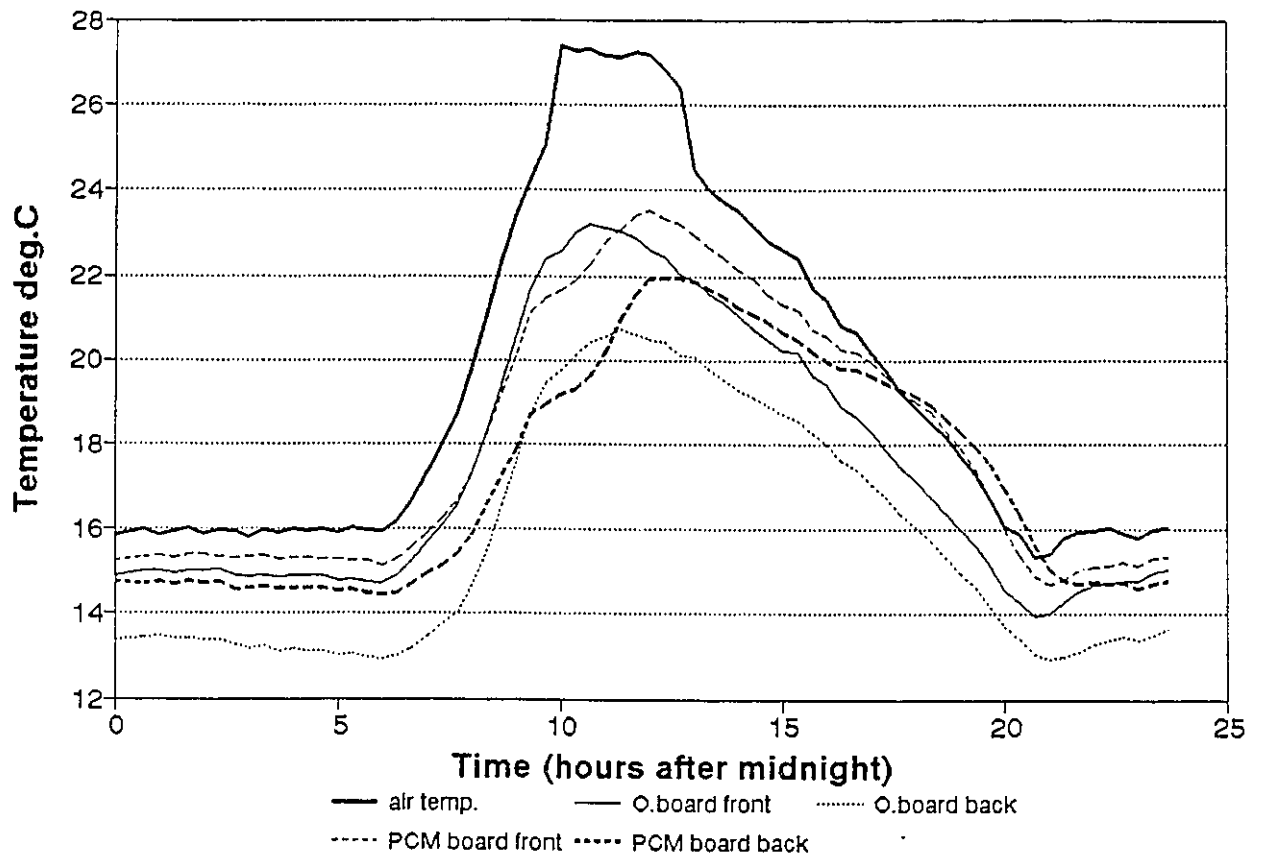


Experimental result for March 9, 92, a mild semi-cloudy day with lowest outside temperature 0 degree. Control strategy: air temperature control, $K_p = 1000 \text{ W./}^\circ\text{C}$, Low setpoint = 16°C , high setpoint = 23°C , high setpoint from hour 7:00 to 17:00.

Figure 3.10 Comparison of the thermal response of the PCM and the ordinary gypsum boards (mild semi-cloudy day, air temperature control with 17:00 to 6:00 night setback)

For semi-cloudy days, the space temperature still increased to as high as 27 °C due to the solar gains, as shown in Figure 3.11 (the setpoint was 23 °C). At this time, even without being directly exposed to solar radiation, the PCM was still melted due to the heat transfer from the room air. Figures 3.12 and 3.13 show a similar phenomenon when the room was heated to 25 °C and 24 °C, respectively, when the room received solar gains. The PCM was melted by the warmed air and excess heat was stored in the melted PCM. These results indicate that the PCM gypsum board can not only absorb direct solar radiation but also the excess heat when the room receives indirect solar gains or is exposed to mild ambient temperature.

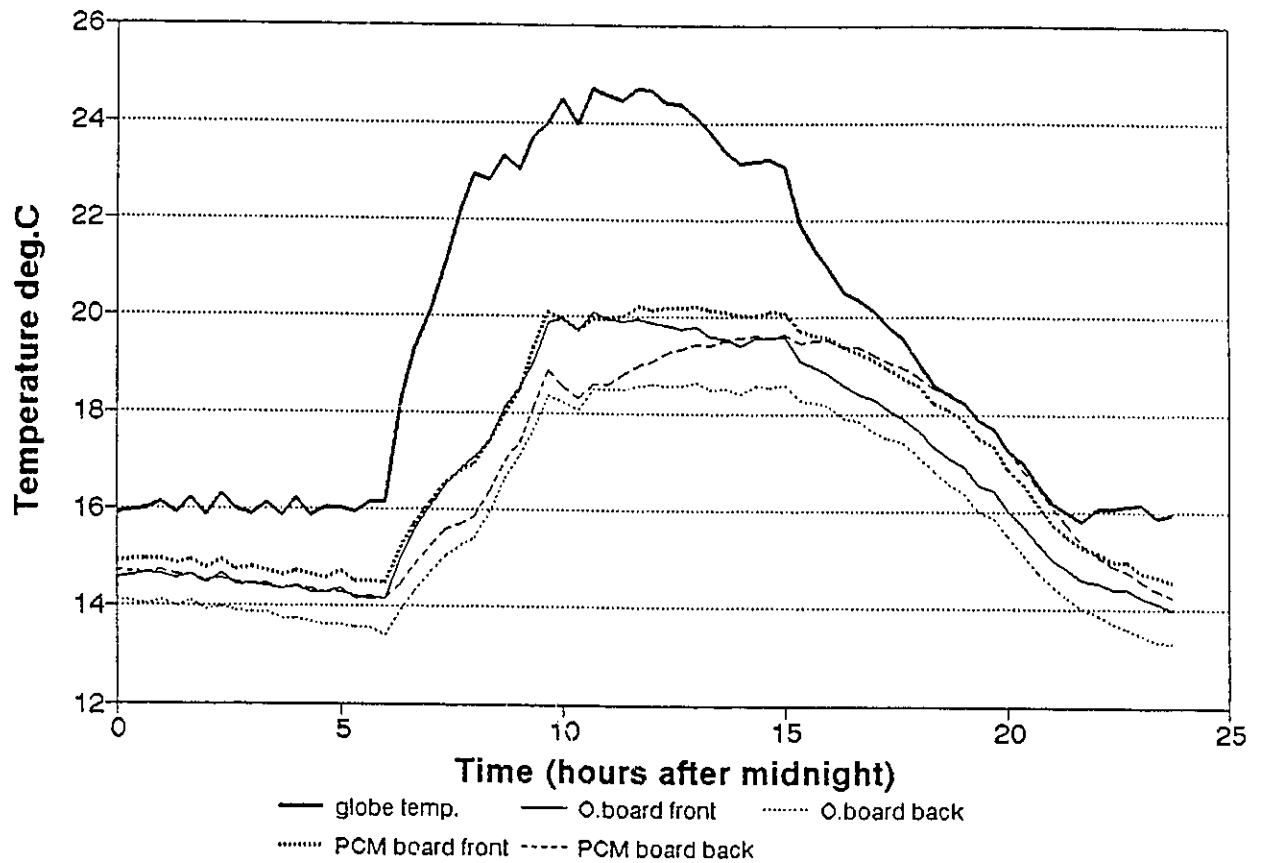
When constant setpoint was used, only the solar gains contributed to the melting and freezing of the PCM. Figure 3.14 shows the thermal response of the PCM and ordinary gypsum board when the setpoint was set at 18 °C constantly during a mild sunny day. As can be seen from the figure, the surface temperature of the PCM board is lower than that of the ordinary board when the room received solar gains (from 9:00 to 13:00). Part of the excess solar gains in the room were stored in the PCM gypsum board during this time. At sunset, the surface temperature of the PCM gypsum board was higher than the ordinary one's because the stored solar gains were being released from the PCM's freezing process. Figure 3.15 shows a similar result obtained from a semi-cloudy day. The thermal response of the PCM and ordinary gypsum board shown in the figures indicates that, when constant setpoint (18 °C) is used, the PCM gypsum board also functions as solar energy storage device during mild sunny and semi-cloudy days.



Experimental result for March 24, 92, a mild semi-cloudy day with lowest outside temperature -7°C and the transmitted solar radiation 500 W/M^2 at noon.

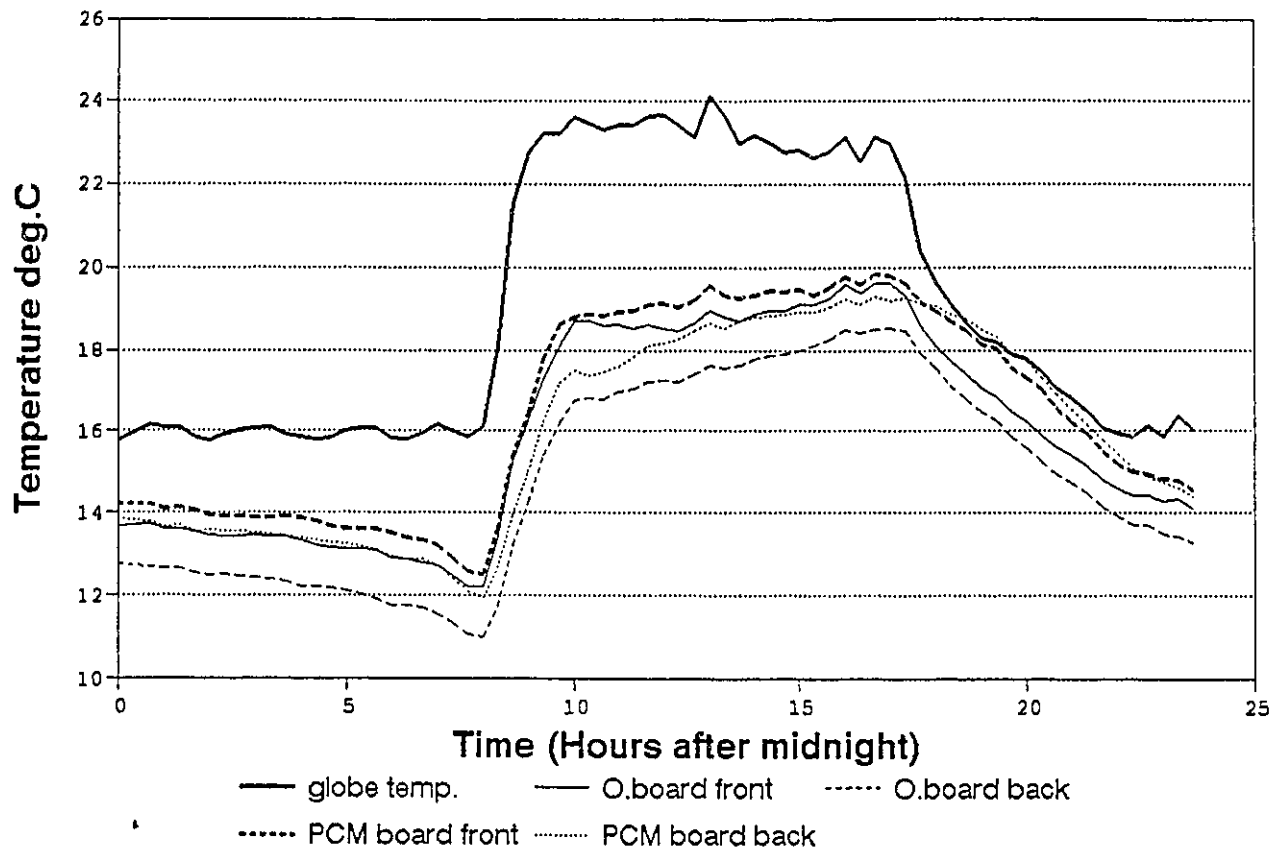
Control strategy: air temperature control, $K_p = 1000 \text{ W/C}$, Low setpoint = 16°C , high setpoint = 23°C , high setpoint from hour 7:00 to 16:00.

Figure 3.11 Comparison of the thermal response of the PCM and the ordinary gypsum boards (mild semi-cloudy day-1, air temperature control with hour 16:00 to 7:00 night setback)



Experimental result for April 8, 92, a mild semi-cloudy day with lowest outside temperature 0°C and transmitted solar radiation 450 W/M².
Control strategy: globe temperature control, $K_p = 1000 \text{ W/C}$, Low setpoint = 16°C, high setpoint = 23°C, high setpoint from hour 7:00 to 16:00.

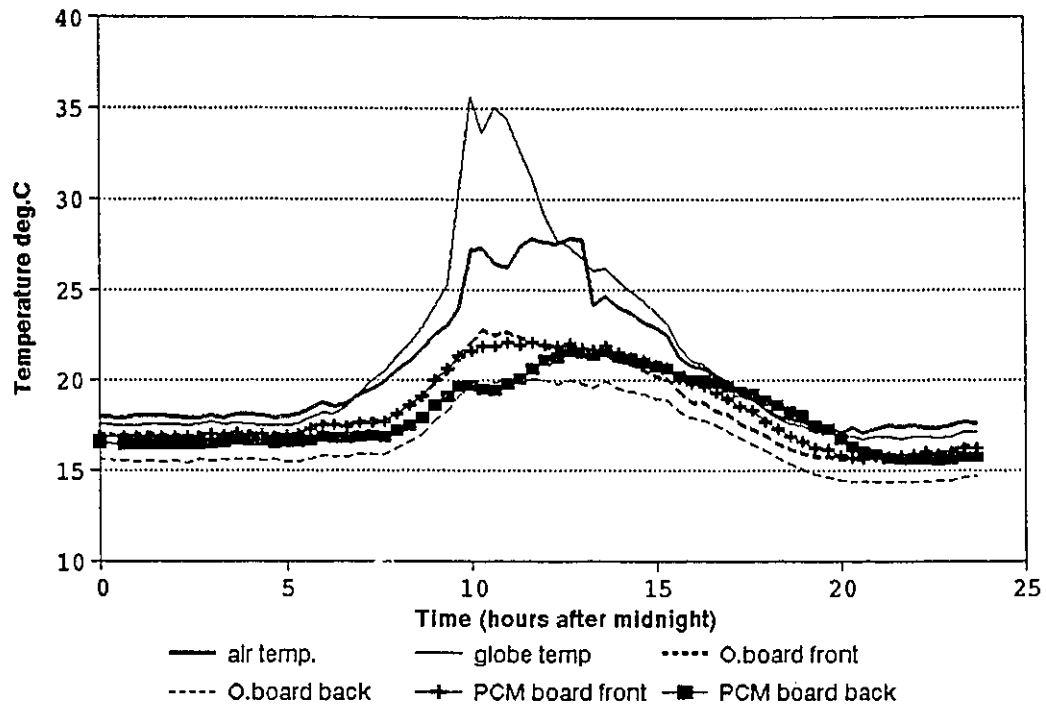
Figure 3.12 Comparison of the thermal response of the PCM and the ordinary gypsum boards (mild semi-cloudy day-2, globe temperature control with hour 16:00 to 7:00 night setback)



Experimental result for April 4, 1992, a mild sunny day with lowest outside temperature -1°C and transmitted solar radiation 490 W/M^2 at noon.

Control strategy: globe temperature control, $K_p = 1000 \text{ W/C}$, Low setpoint = 16°C , high setpoint = 23°C , high setpoint from hour 7:00 to 16:00.

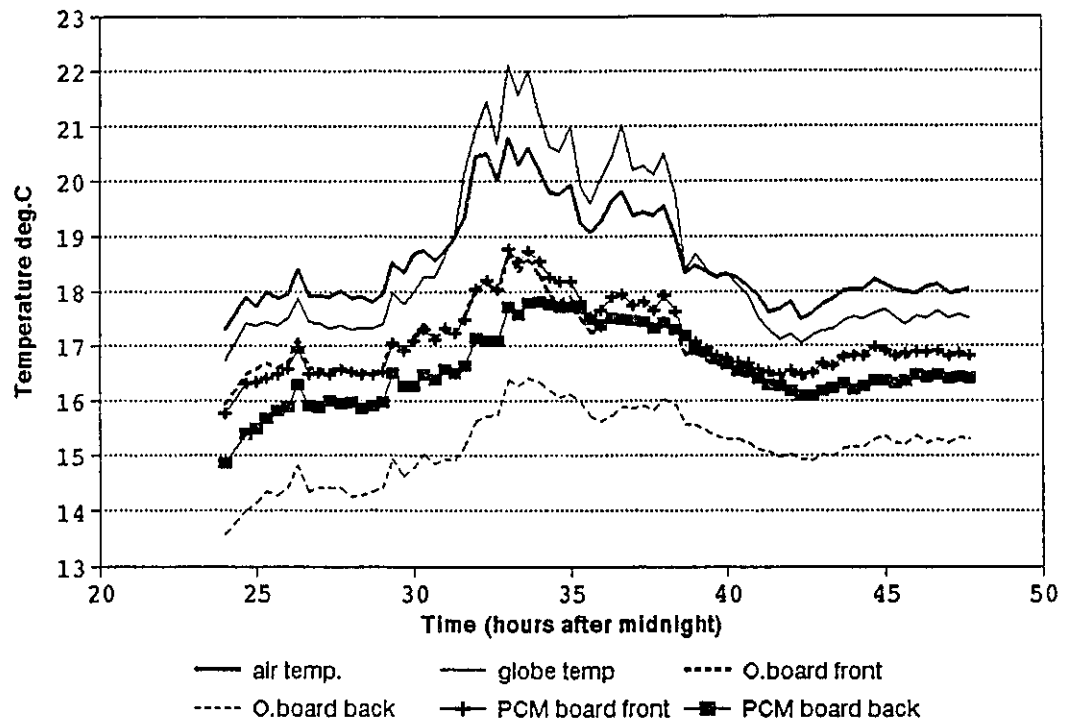
Figure 3.13 Comparison of the thermal response of the PCM and the ordinary gypsum boards (mild semi-cloudy day-3, globe temperature control with hour 16:00 to 7:00 night set back)



The experiment was performed on March 22, 1993, a mild sunny day with an outside temperature range of -2°C to 0°C and outside solar radiation 900 W/m²;

Control strategy: air temperature control, constant setpoint at 18°C.

Figure 3.14 Comparison of the thermal response of the PCM and the ordinary gypsum boards (mild sunny day, air temperature control with constant setpoint)



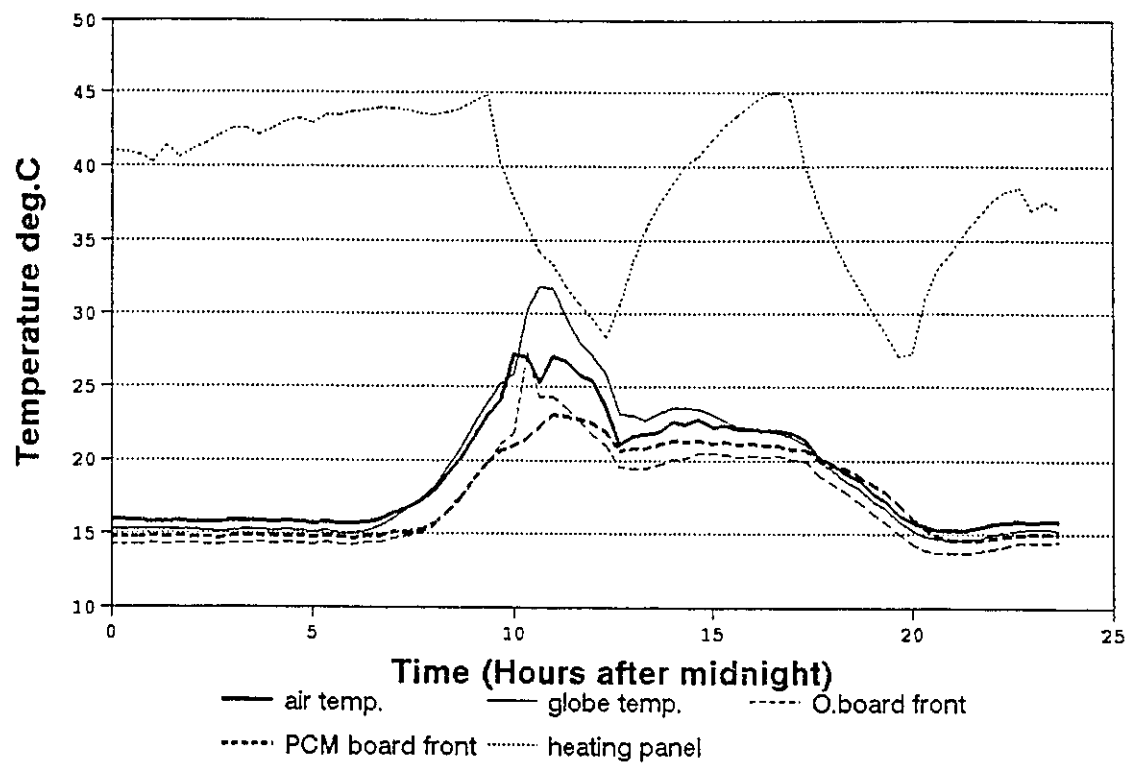
The experiment was performed on March 20, 1993, a mild semi-cloudy day with an outside temperature range of -7°C to -1°C and outside solar radiation 500 W/m^2 ; Control strategy: air temperature control, constant setpoint at 18°C .

Figure 3.15 Comparison of the thermal response of the PCM and the ordinary gypsum boards (mild cloudy day, air temperature control with constant setpoint)

Reduction of overheating

Figure 3.16 shows an experimental result obtained from a cold sunny day. In the figure, the front surface temperature of the PCM gypsum board was generally lower than the globe temperature when the test room received solar gains and the heating panel was off. This indicates that the PCM gypsum board functions as a cooling surface when the overall space temperature is higher than the setpoint.

As can be seen from the figure, from morning through noon, inside room air temperature increased due to the change of setpoint and the increase of solar radiation. When the air temperature increased as high as approximately 26 °C, the melting of the PCM started to affect the air temperature. At this time, the room air temperature tends to decrease instead of continually increase because a large amount of heat was absorbed by the PCM's melting process. This phenomenon can also be found from previously presented results obtained from sunny days (Refer to Figure 3.5, 3.6 and 3.7). As indicated by the previous analysis of the thermal response of the PCM gypsum board, under direct solar radiation, the front surface temperature of the PCM gypsum board was lower than the ordinary one's two to six °C, and the amount was one to two °C when no direct solar radiation was exposed by the boards. The lowered PCM gypsum board surface temperature contributes to the reduction of room overheating. A previous work [7] (Athienitis, 1992) showed that, when no PCM wallboard was employed in the test-room, room air temperature was often as high as 30 °C during a sunny day, while it was 25-26 °C after the PCM wallboard was used (with the similar weather conditions). A significant conclusion is that the application of PCM gypsum board can effectively restrict overheating in a passive solar room.



Experimental result on March 15,1992, a cold sunny day with lowest outside temperature -15 C and transmitted solar radiation 600 W/M²

Control strategy: air temperature control, $K_p = 1000 \text{ W/C}$, Low setpoint = 16 C, high setpoint = 23 C, high setpoint from hour 6:00 to 17:00.

Figure 3.16 Thermal performance of the test room

Improvement of the thermal comfort

Previous analysis of the thermal response of the PCM gypsum board also showed that the surface temperature change of the PCM wallboard is restricted when the space temperature changes significantly due to solar gains. Since the PCM wallboard constitutes more than half of the total interior surface of the test room, its smooth surface temperature variation helps to provide a slower globe temperature change. Considering that the globe temperature is one of the most important parameters indicating the human thermal comfort conditions, the use of the PCM gypsum board can effectively improve the thermal comfort level. When the space receives much solar radiation, the outside temperature change rapidly or internal gains vary significantly, the space globe temperature can be moderated when the PCM wallboard is used as wall interior lining.

Storage of extra heat and its reuse

The experimental results also reveal that the thermal energy stored as latent heat in the melted PCM during the daytime can be released from the PCM's freezing when the ambient temperature decreases at night. Released energy from the freezing process delays the cooling of the room air. As an example, the result from the experiment on March 15, 1992 (Figure 3.10) shows that during the freezing process which lasted 4.5 hours, the PCM gypsum board front surface temperature is on average 2.5 °C higher than that off the ordinary board. With a total of 19.69 m² PCM gypsum board used in the test room, the latent heat released from the 4.5 hours' freezing process reduced the heating load by 6.5×10^6 Joules. In 4.5 hours, this amount is equivalent to a 403 watts' auxiliary electrical heating, approximately 30% of the peak heating

load. This estimation was conducted as follows:

$$\text{Reduced heating load} = h_{in} \cdot \Delta T \cdot A$$

where, h_{in} = inside film coefficient (8 W/m²);

ΔT = average temperature difference between ordinary and PCM boards
(2.56 °C);

A = surface area (19.69 m²).

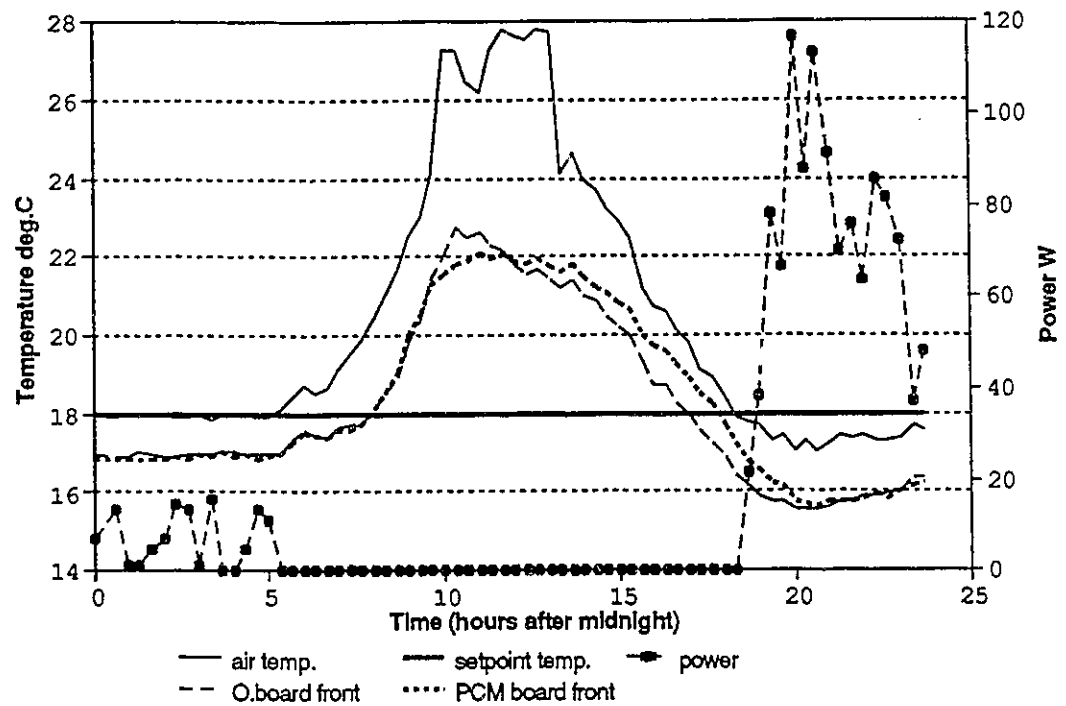
The conclusion is that extra heat can be stored in the PCM gypsum board during daytime and can be utilized at night. Building energy efficiency is thus improved.

Advance of the setpoint setback

In experiments No.9, No.10 and No.11 (refer to Figure 3.11, 3.12 and 3.13), when the weather was not extremely cold (the lowest outside temperature was higher than -10 °C), the time for setting back the space setpoint, from 23 °C to 16 °C, was advanced from hour 17:00 to 16:00. The results showed that the air temperature or the globe temperature was still maintained above 18 °C until 17:00 in all these days. This is because the released energy from the PCM's freezing process prevents fast drop of the room temperature, especially the globe temperature. The strategy can be used to reduce the heating energy consumption by setting back the setpoint before the vacancy of the building and maintain an acceptable space thermal comfort level.

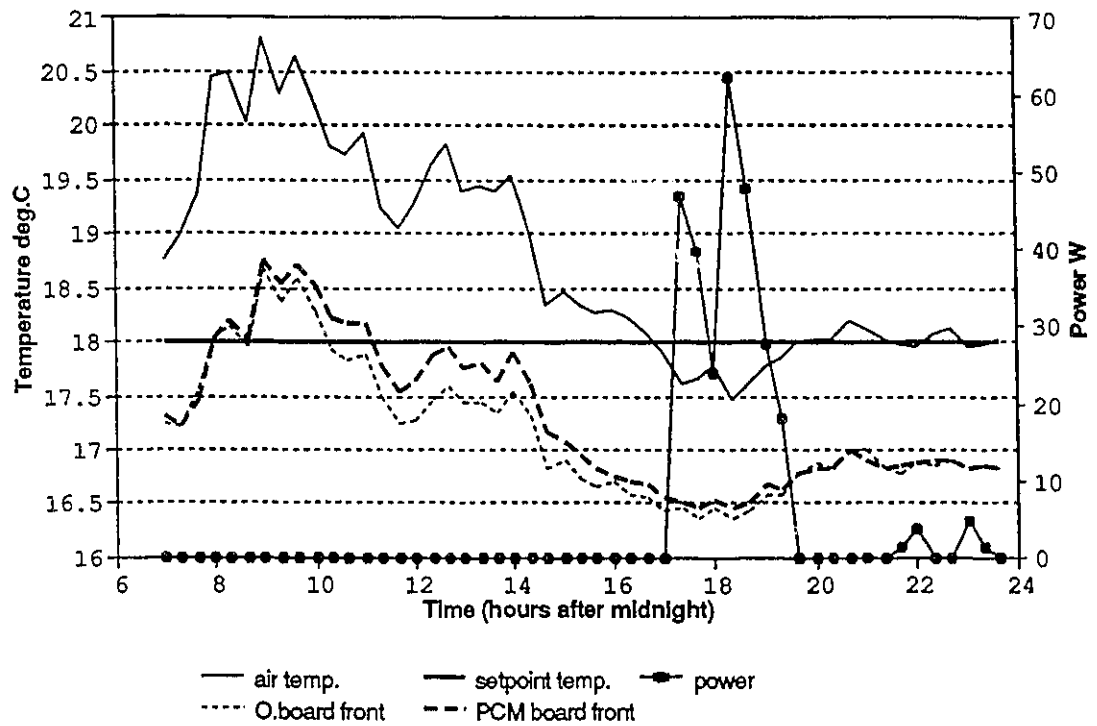
It can be estimated that, during the evening after a mild-sunny day, (it often happens in the early spring and late autumn), the required space temperature can be maintained mainly by reuse of

the latent heat stored during the daytime. Figures 3.17 and 3.18 show the off-heating periods during which the room temperature was kept in the comfort range by solar gains and the released latent heat. In Figure 3.17, the off-heating period was from hour 5:10 to 18:30 (11.2 hours) on a mild sunny day. In Figure 3.18, it was from 7:00 to 17:00 (ten hours) in a mild cloudy day.



The experiment was performed on March 22, 1993, a mild sunny day with an outside temperature range of -2°C to 0°C and outside solar radiation 900 W/m²; Control strategy: air temperature control, constant setpoint at 18°C.

Figure 3.17 Auxiliary heating and room temperature with PCM wallboard installed (mild-sunny day)



The experiment was performed on March 20, 1993, a mild semi-cloudy day with an outside temperature range of -7°C to -1°C and outside solar radiation 500 W/m^2 ; Control strategy: air temperature control, constant setpoint at 18°C .

Figure 3.18 Auxiliary heating and room temperature with PCM wallboard installed (mild-cloudy day)

CHAPTER 4 MATHEMATICAL MODEL

4.1 INTRODUCTION

The conclusions from the experimental results are that by use of the PCM gypsum board in the test room, the room overheating can be reduced during the PCM's melting process and a significant amount of heat is released during its freezing process. However, the experimental result is not enough to perform the estimation of the effect of the PCM wallboard under the circumstances which are different than the ones existing in the test-room. More investigation is required to study the thermal performance of the PCM gypsum wallboard when applied in different types of buildings, with a variety of given setpoint and weather conditions. The work also should be extended to the study of the adaptive thermal control strategies and the reduction of furnace cycling. It is not necessary or feasible to perform all these studies experimentally. Alternatively, an effective mathematical model is required for further research and design.

4.2 PREVIOUS MODELS

Mathematical solutions have been devised for heat transfer problems in the materials which undergo phase changes in a given temperature range, especially since the late 1970's. These mathematical models were mainly classified into two categories. One is the analytical solution and the other is the numerical solution. In the analytical one, Ozisik (1979) dealt with an infinite medium with cylindrical symmetry [20]. A publication "Transient Heat Transfer Analysis of

Alloy Solidification" by Muehlbauer, Hatcher and Sunderland (1973), [23], presented an approximate mathematical analysis obtained for the temperature distribution and rate of phase change for the transient one-dimensional solidification of a finite slab of a binary alloy. However, these previous analytical solutions dealt with simple boundary conditions, such as the first or second class boundary conditions. During the present study, many efforts have been made to find the analytical solutions for a finite slab problem with the third class boundary conditions. But the equations with λ and η (the ratio of liquid-mushy and mushy-solid boundary location to time, refer to Ozisik (1979), [20]) were found with variable t (time) involved explicitly. The analytical approach is very complicated for the simulation of the heat transfer process in the PCM wallboard exposed to the boundary conditions with transient convective and radiative heat source such as those involved in a passive solar room.

Many numerical solutions have been successfully applied, even to very complicated heat and mass transfer problems in which the substance may involve phase transition in a given temperature range. Morgan (1981) presented an explicit finite element algorithm for the solution of the basic equations describing combined conductive and convective transfer with phase change involved [21]. In addition, Voller and Prakash (1987) developed an enthalpy formulation based on fixed grid methodology for the numerical phase change problems [22]; Cao, Faghri and Juhasz (1991) solved the change of phase of PCM and the transient forced convection heat transfer simultaneously as a conjugate problem [24]. Kedl (1991), [13], studied the thermal performance of the PCM wallboard with surface temperatures controlled on both sides, both experimentally and theoretically. The mathematical modelling and experimental results agreed well in his work.

Based on a survey of previous works, a numerical solution is chosen for the following reasons:

1. It is adaptable to apply to different kinds of boundary conditions which could arise in actual building applications.
2. It is easily modified so that the thermal performance of other PCM building materials, such as PCM concrete block, can be modelled as well.

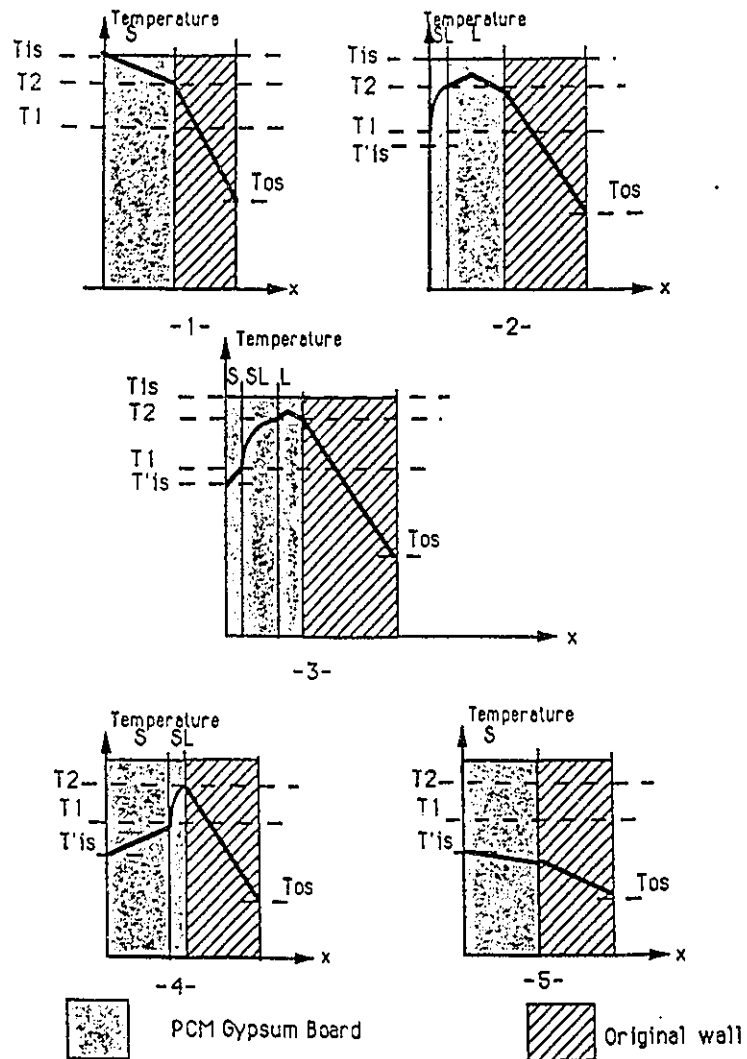
4.3 MODELLING ASSUMPTIONS

The heat transfer mechanism is complex in PCM gypsum board, especially when the PCM is at its phase transition stage. Figure 4.1, a conceptual diagram shows the temperature transition profiles across the PCM board during its freezing process. The initial condition assumed is that the room air temperature is higher than 22 °C and the PCM in gypsum board is in the liquid phase. As the room air temperature cools, the solidification process starts from the cooler edge (left edge in Figure 4.1) of the PCM board. The PCM in the wallboard changes from a liquid state to a mushy one and then it becomes solid. As the temperature of the cooler side continues to decrease, the mushy state goes forward from the cooler side to the warmer side and the solid band becomes progressively wider until all the PCM in the gypsum board becomes solid. When the PCM in the gypsum board undergoes a phase change, the densities of the three states (solid, mushy and liquid) of the PCM gypsum board are different. The density difference causes natural convection at the boundary of the mushy and liquid states. In addition, the physical and thermal properties of the PCM in the gypsum pores are also different. If all these factors are taken into account, the study could become very complicated for practical analysis. To simplify the process,

three assumptions are made:

1. The natural convection at the mushy-liquid boundary is neglected because the density difference between the mushy and liquid states is small and the convective effect is significantly reduced due to the flow resistance caused by the gypsum pores.
2. PCM and gypsum matrix are considered as a uniform body. Furthermore, this uniform body is considered to have integrated physical and thermal properties, such as specific heat, density, thermal conductivity and latent heat. These integrated properties have been obtained directly from the Differential Scanning Calorimeter (DSC) test. Many previous studies such as Ozisik (1979), [20], and Morgan (1981), [21], have proved that this assumption does not affect the results significantly.
3. The heat transfer process across the PCM gypsum board and the original wall is treated as a one-dimensional problem. The justification for this is that the temperature difference across the wall is much larger than it is along the wall and the dimension across the wall is very small compared with the dimension along the wall (the ratio is 1/20). The heat transfer along the wall may, therefore, be neglected because of the small temperature difference and the large thermal resistance.

Based on the above assumptions, the heat transfer problem across the wall is treated as a one dimensional, transient heat diffusion problem with uniform physical and thermal properties and a temperature dependant heat source which represents latent heat flow.



- * T_{1s} and T'_{1s} are the inside air temperatures, $T_{1s} = 23^{\circ}\text{C}$, $T'_{1s} = 16^{\circ}\text{C}$
- * S = Solid state, SL = mushy state, L = Liquid state

Figure 4.1 Conceptual temperature distribution across PCM gypsum board during freezing process

4.4 GOVERNING EQUATIONS

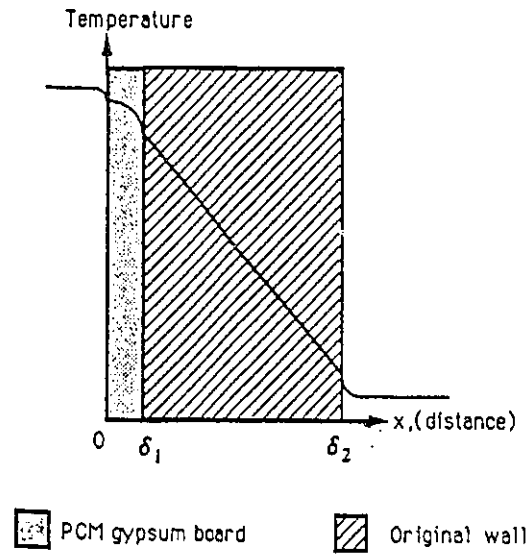


Figure 4.2 Schematic of heat transfer system for mathematical model

Figure 4.2 shows the temperature decreasing across a wall with PCM gypsum board as inside lining. One surface of the PCM wallboard is exposed to inside air and the other abuts the original wall. The energy balance for the heat transfer system shown in Figure 4.2 is governed by the one dimensional heat diffusion equation:

$$\rho C_p \frac{\partial T(x,t)}{\partial t} = k \frac{\partial^2 T(x,t)}{\partial x^2} + q(x,t) \quad (4.1)$$

with boundary conditions:

$$-k \cdot \frac{\partial T(x,t)}{\partial x} = h_i(t) \cdot (T_{air}(t) - T(x,t)) + \alpha q_s(t) \quad x=0 \quad (4.2)$$

$$-k \cdot \frac{\partial T(x,t)}{\partial x} = h_{out} \cdot (T_o(t) - T(x,t)), \quad x=\delta_2 \quad (4.3)$$

where,

- ρ = density, kg/m³, when $0 \leq x \leq \delta_1$, it is the density of PCM gypsum board; when $\delta_1 \leq x \leq \delta_2$, it is the density of the original wall;
- C_p = specific heat, J/kg.K, when $0 \leq x \leq \delta_1$, it is the specific heat of the PCM gypsum board, when $\delta_1 \leq x \leq \delta_2$, it is the specific heat of the original wall;
- k = thermal conductivity, W/m.°C, it equals to the thermal conductivity of PCM gypsum board when $0 \leq x \leq \delta_1$, and the thermal conductivity of the original wall when $\delta_1 \leq x \leq \delta_2$;
- $T(x,t)$ = temperature of concerned element, °C,;
- $T_{air}(t)$ = inside air temperature, °C;
- $T_o(t)$ = outside air temperature, °C;
- x = distance from origin of x axis, m;
- t = time, s;
- $q(x,t)$ = latent heat flow when phase change occurs at $0 < x < \delta_1$, W/m³; It equals zero at $\delta_1 \leq x \leq \delta_2$;

$h_{in}(t)$ = transient inside film coefficient, $W/m^2 \cdot ^\circ C$, it is determined by radiative and convective heat change between inside air and board inside surface (refer to Appendix-C);

h_{out} = outside film coefficient, $W/m^2 \cdot ^\circ C$.

α = surface solar absorptivity;

$q_s(t)$ = intensity of the solar radiation incident on the surface at $x = 0$, $W/m^2 \cdot ^\circ C$, which is determined as follows:

$$q_s(t) = \begin{cases} 0 & t < T_{sr} \\ q_{sp} \sin\left[\frac{\pi}{T_{ss} - T_{sr}} (t - T_{sr})\right] & T_{sr} \leq t \leq T_{ss} \\ 0 & t > T_{ss} \end{cases} \quad (4.4)$$

where,

q_{sp} = the peak value of solar radiation intensity, W/m^2 ;

t_{sr} = sunrise time on the surface, s;

t_{ss} = sunset time from the surface, s.

4.5 DETERMINATION OF LATENT HEAT FLOW

In constructing a solution to a heat transfer problem involving a liquid/solid change of phase, a key factor is to correctly simulate the latent heat flow, term $q(x,t)$ in equation (3.1), then to solve

equations (3.1) to (3.3).

4.5.1 PREVIOUS MODELS

The latent heat flow indicates the rate of latent heat generation per unit mass of PCM at a specific temperature $T(x,t)$. It can be simulated by two methods. One is the "enthalpy method" and the other is the "temperature-based equivalent heat capacity method". The former one, used by Ozisik (1979), [20], Voller and Prakash (1987), [22], simulates the heat released from solidification as a volumetric heat generation term,

$$q(x,t) = \rho L \frac{df_s}{dt} \quad (4.5)$$

where,

ρ = density of the PCM;

f_s = solid fraction in the two-phase region at the solidus front, it depends on the substance's composition;

L = the value of latent heat, given unit mass of PCM during a freezing or melting process, J/kg;

t = time, s.

In the temperature-based equivalent heat capacity method, the amount of latent heat is transformed to the form of a substance's heat capacity as a function of its temperature as

follows:

$$C = C(T^*) = \begin{cases} C_s & (T^* < -\delta T) \\ C_m + \frac{H}{2\delta T} & (-\delta T \leq T^* \leq \delta T) \\ C_l & (T^* > \delta T) \end{cases} \quad (4.6)$$

where,

ρ = density of the PCM, kg/m^3 ;

C = specific heat, $\text{J/K} \cdot ^\circ\text{C}$;

T = temperature, $^\circ\text{C}$;

H = latent heat, J/Kg ;

C_s = thermal capacity of solid state;

C_l = thermal capacity of liquid state;

C_m = thermal capacity of mushy state;

T^* = scaled temperature .

This method had been successfully used by Cao and Faghri (1991) in their relevant work [24] previously mentioned and it can effectively eliminate the effects of time step and grid size which are normally encountered for other fixed-grid methods. However, this problem only exists when natural or forced mass flow is involved. For the present study without mass flow involved, as assumed, fix-grid method can be chosen and the enthalpy method is chosen as a result.

4.5.2 DSC TEST

The value of latent heat 'L' and the rate of solidification ' df_s/dt ' in equation (4.5) were obtained from the Differential Scanning Calorimeter (DSC) test. Referring to Figure 4.3, the DSC test consists of heating/cooling a weighted sample and an empty reference sample pan both at the same controlled rate, R, in an insulated chamber. If a given heat exchange related to the phase change takes place in the sample, but not in the empty reference pan, the resulting difference in the temperature between them is directly related to the heat flow to or from the sample. This differential heat flow is quantitatively measured and plotted in the form of DSC curves as shown in Figure 4.4. The value of the latent heat, L, flow from or to the sample is calculated by automatic peak integration of the related heat flow vs time curves.

The DuPont 910 DSC consists of a cell base module which is directly connected to a programmer-recorder (1090 DuPont) thermal analyzer. The parameters which are calculated by the interactive Data Analysis Program are the following: (referring to Figure-4.4):

a) Melting point and freezing point

The initial melting point or freezing point onset temperature on the heating or cooling curve is the calculated temperature at the intersection of the base line with the tangent to the inflection point in the curve of heat flow versus temperature;

b) Heat of melting and freezing

The heats of melting and freezing are calculated from the integrated area over time for the heat flow associated with melting (an endothermic process) or freezing (an exothermic

process) based on the following formula:

$$L = \frac{k}{m} \times \int_{t_1}^{t_2} \frac{\Delta Q}{f(T)} dt \quad (4.7)$$

where,

L = heat of phase transition;

m = sample mass;

ΔQ = heat flux;

t = time;

k = DSC constant (obtained by calibration)

$f(T)$ = temperature dependent heat transfer function.

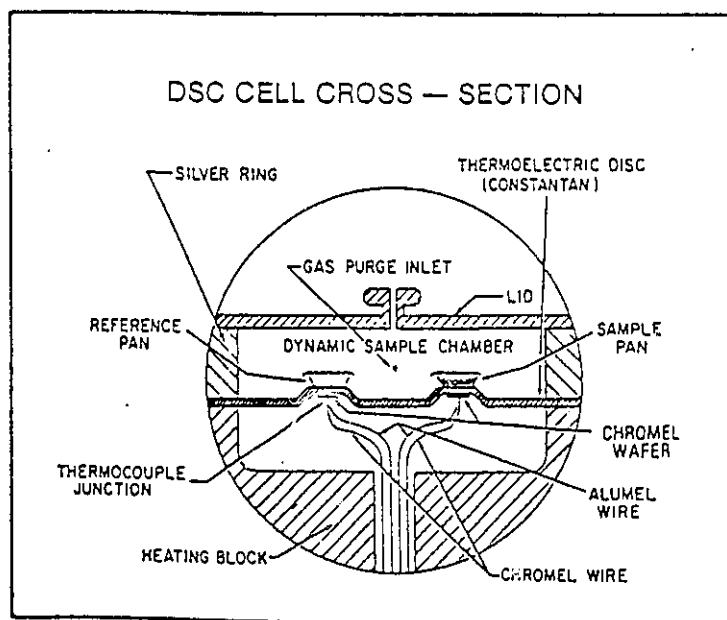
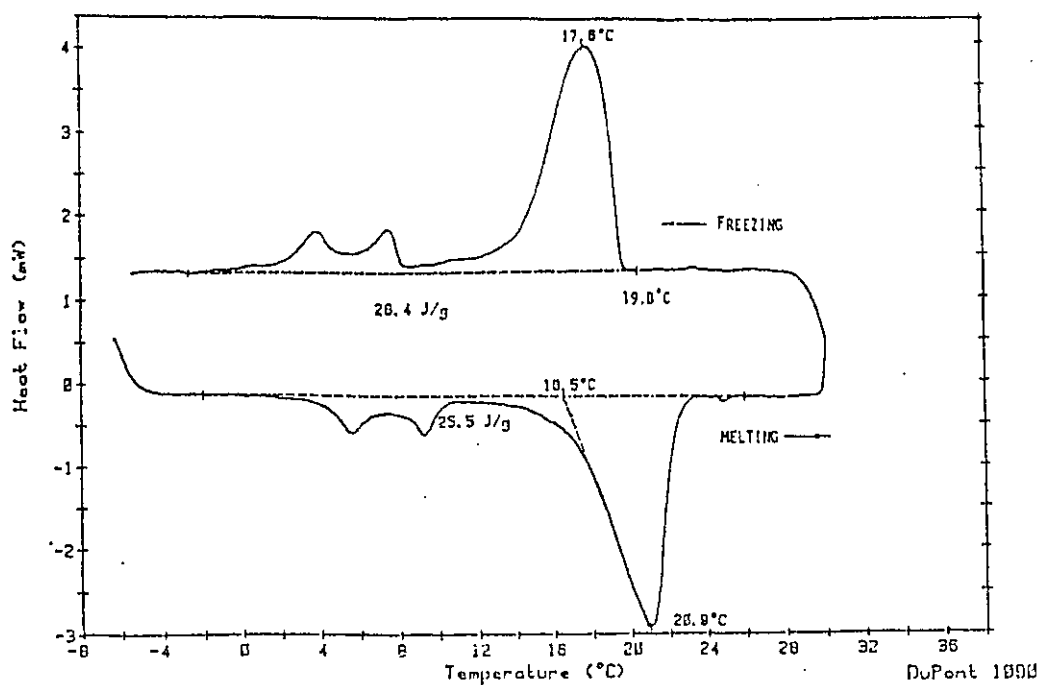


Figure 4.3 The DSC Test (from reference [5])

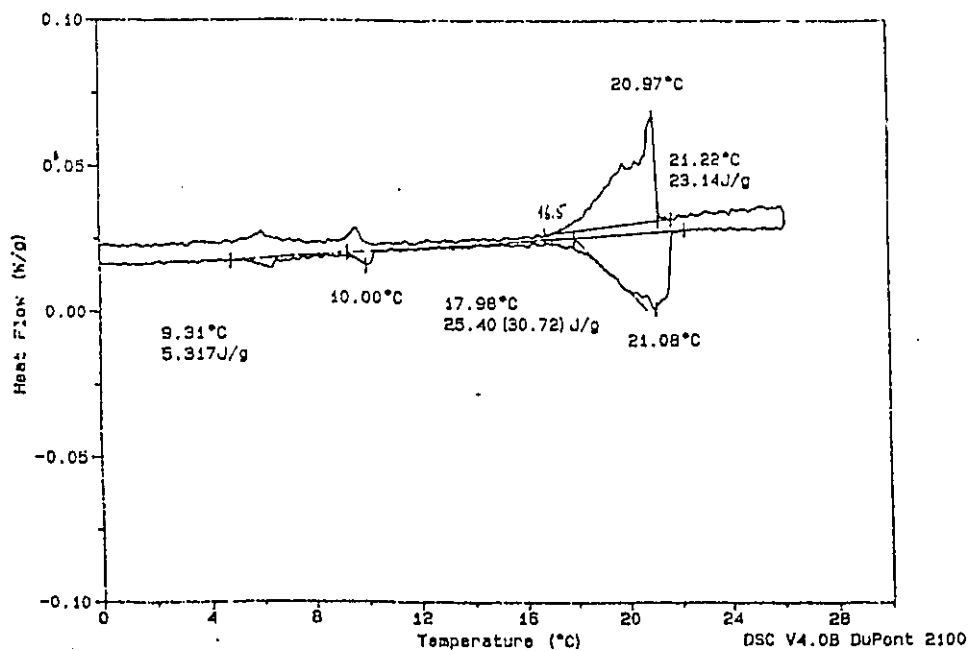
Examination of all the DSC curves presented in "Energy Storing Wallboard" [5] revealed that the latent heat value, L , is affected by the following factors (refer to Figure 4.4):

- a) the type of phase change material and the percentage of incorporation;
- b) the size of sample;
- c) heating or cooling rate of the DSC test.

Figure 4.4 (a) and (b) shows the difference of the DSC curves obtained from two DSC tests with the same test conditions except the different heating/cooling rate, 0.15 °C/min and 2 °C/min.



(a)



(b)

Figure 4.4 DSC test results of BS-gypsum board, (a) with testing rate 2°C/min; (b) with testing rate 0.15°C/min

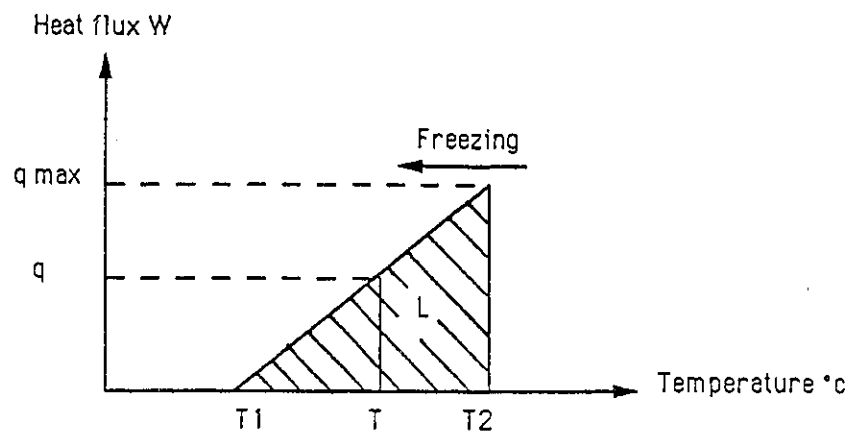


Figure 4.5 A schematic diagram for DSC curve

Satisfactory simulation of the latent heat flow can be achieved only after these factors are taken into account. The simulation was performed according to the DSC test which possessed the following features:

- the sample contained 24.8 wt% butyl stearate in the gypsum board, as used in the present study;
- size of sample is 26.678 mg weight, the diameter is around 1-2 mm;
- the heating or cooling rate is 0.15 °C/min, which approximates the rate of temperature change in the test room.

4.5.3 SIMULATION OF THE LATENT HEAT FLOW

A DSC curve, as shown in Figure 4.4 (b), was chosen based on the former consideration and modelled by a schematic diagram shown in Figure 4.5. In the figure, T_2 and T_1 respectively indicate the temperatures at which freezing process starts and ends. q_{\max} indicates the maximum latent heat flow. The area of triangle $T_1 T_2 q_{\max}$ is the value of latent heat, L . With known heating or cooling rate, R , we have:

$$L = \frac{1}{2} q_{\max} (T_2 - T_1) \cdot \frac{1}{R} \quad (4.8)$$

where,

- L = latent heat for a whole freezing or melting process in the DSC test (it is in a temperature range of -2 to 32 °C in the present study), J/g;
- R = heating or cooling rate, °C/second;
- T_1, T_2 = the initial melting and freezing points, respectively.

From simple trigonometry, the latent heat flow, $q(x,t)$, is thus determined as:

$$q(x,t) = \frac{T - T_1}{T_2 - T_1} q_{\max} \quad (4.9)$$

Substituting (4.8) into (4.9), we obtain:

$$q(x,t) = 2 \cdot L \cdot R \cdot \frac{T - T_1}{(T_2 - T_1)^2} \quad (4.10)$$

Through examination of the DSC curves, it is also found that a correct must be made as follows:

$$L_p = (60\% - 65\%) \cdot L \quad (4.11)$$

where, L_p = latent heat given by the PCM when phase transition occurs in the temperature range of T_1 to T_2 .

Replace L with L_p in equation (4.10), latent heat flow is thus determined as:

$$q(x,t) = 2 \cdot L_p \cdot R \cdot \frac{T(x,t) - T_1}{(T_2 - T_1)^2} \quad (4.12)$$

Similarly, the latent heat flow absorbed by a melting process is determined by:

$$q(x,t) = -2 \cdot L_{pm} \cdot R \cdot \frac{T(x,t) - T_1}{(T_2 - T_1)^2} \quad (4.13)$$

where, L_{pm} = latent heat absorbed by a melting process occurs in the temperature range of T_1 to T_2 .

4.6 FINITE DIFFERENCE THERMAL NETWORK MODEL

The outlined mathematical model for dealing with the transient heat diffusion across the PCM gypsum board was solved with an explicit finite difference method. As shown in Figure 4.6, to

perform this finite difference solution procedure, the heat transfer system is modelled by a 19-node thermal network. In the thermal network, nodes 2 to 15 represented the PCM gypsum board. Nodes 16 to 18 represented the original wall construction. Node 1 and node 19 represented the inside and outside air respectively. Parameters of the thermal network model are given in Appendix A. Based on this thermal network model, for node 3-17, equation (4.1) (for heat diffusion) is written in a finite difference form as follows:

$$T_i^{p+1} = \frac{\Delta \tau}{C_i} * [q_i + \sum_j \frac{T_j^p - T_i^p}{R_{ij}}] + T_i^p \quad (4.14)$$

For node 2 and node 18, the equations (3.2) and (3.3) (for boundary conditions) are given by:

$$T_2^{p+1} = \frac{T_1^p h_\epsilon^p + T_3^p / R_{23} + \alpha q_s^p}{h_\epsilon^p + 1/R_{23}} \quad (4.15)$$

$$T_{18}^{p+1} = \frac{(1/R_{17,18}) T_{17}^p + h_{out} T_{19}^p}{h_{out} + 1/R_{17,18}} \quad (4.16)$$

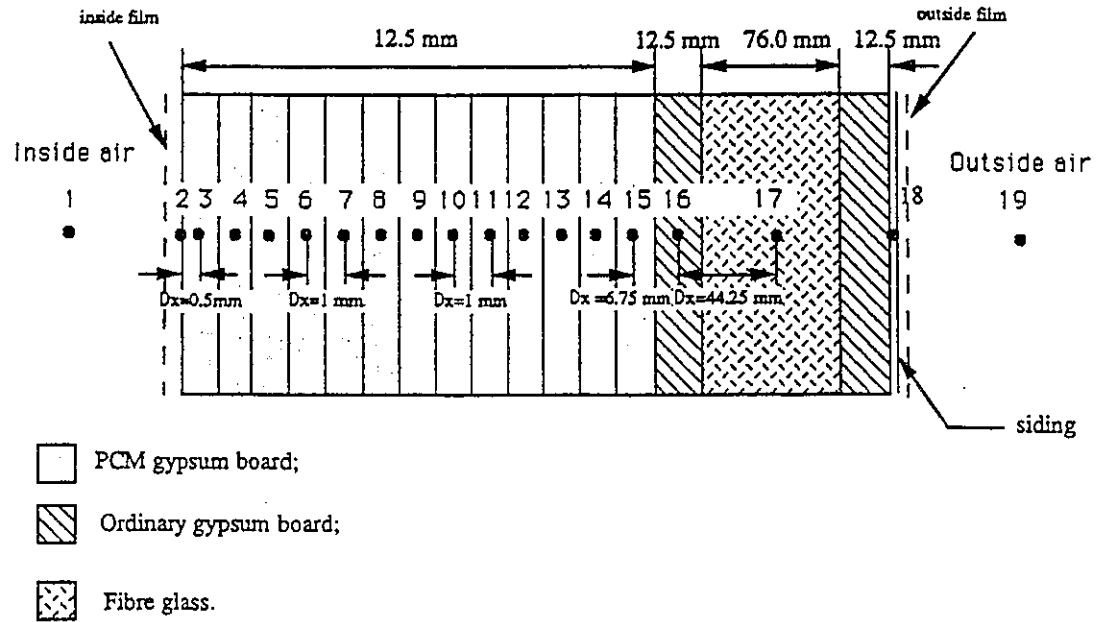
where,

T_i^{p+1} = the temperature of node i at time step p+1, °C;

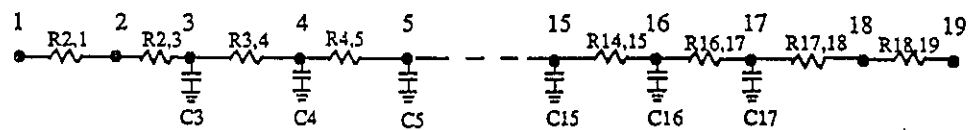
T_i^p = the temperature of node i at time step p, °C;

T_j^p = the temperature of an adjacent node to node i, node j, at time step p, °C;

4.6 FINITE DIFFERENCE THERMAL NETWORK MODEL



(a)



(b)

Figure 4.6 *Finite difference system, a) the physical system and nodal arrangement; b) thermal network model*

- q_i^p = latent heat flow released or absorbed by node i at time p, watt;
 C_i = heat capacity of node i, J/K;
 R_{ij} = the thermal resistance between node i and its adjacent node j, K/W;
 $\Delta\tau$ = time step, s;
 q_s^p = intensity of incident solar radiation at time p, W/m²;
 α = surface absorptivity;
 h_{in}^p = inside film coefficient at time p, W/m².°C;
 h_{out} = outside film coefficient, W/m².°C
 subscript
 i = the node number, from 1 to 19;
 j = the number of the adjacent node to node i;
 superscript
 p = the time step number, from 1 to n seconds, 'n seconds' is the duration of freezing or melting procedure concerned in the simulation.

The time step is determined to satisfy the stability requirement by:

$$\Delta\tau \leq \left[\frac{C_i}{\sum_j \left(\frac{1}{R_{ij}} \right)} \right]_{\min} \quad (4.17)$$

The minimum time step which is required by node 15 is 2.71 seconds. A 1 second time step thus

satisfied the stability requirement and was chosen in this explicit finite difference model.

The simulation was also performed for the ordinary gypsum board with the same given boundary conditions. Through the comparison between the simulations for the PCM and the ordinary gypsum boards, the amount of potential energy saving (the reduction of heating load) from the application of PCM gypsum board was obtained by:

$$\overline{Q_{es}} = \frac{1}{t} \int_0^t [h_{sp}(T_{isp} - T_a) - h_{so}(T_{iso} - T_a)] dt \quad (4.18)$$

where,

Q_{es} = average energy saving from unit area of the PCM board during freezing time period t , W;

h_{so} = inside surface film coefficient for ordinary board, W/m^2 ;

h_{sp} = inside surface film coefficient for PCM board, W/m^2 ;

T_{iso} = inside surface temperature of ordinary board, $^{\circ}C$;

T_{isp} = inside surface temperature of PCM board, $^{\circ}C$;

T_a = inside air temperature, $^{\circ}C$.

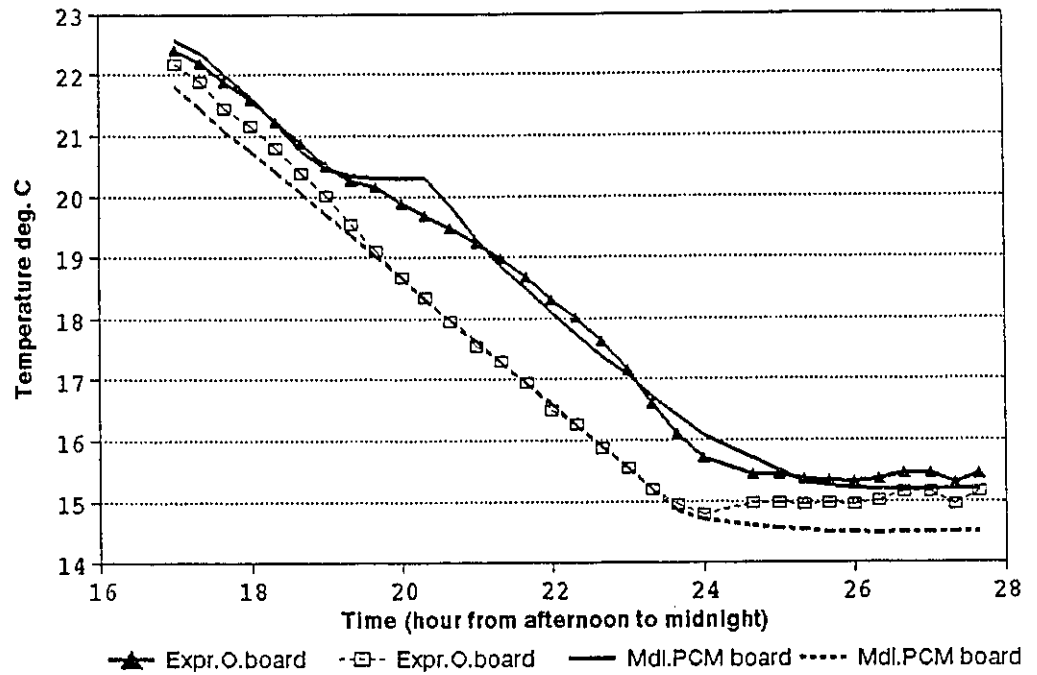
A FORTRAN program named "PCMBOARD" was developed based on this finite difference model. Using the program, the transient board surface temperatures and the amount of release or absorption of latent heat can be calculated with a variety of given conditions, such as solar radiation and transient inside/outside temperatures.

4.7 NUMERICAL EXPERIMENTS AND RESULTS

The program was tested by performing a series of simulations. Figures 4.7 and 4.8 show the comparison between the numerical and experimental results for a freezing and a melting process, respectively. In Figures 4.7 and 4.8, "Mdl.PCM board" and "Mdl.O.board" represent the mathematical model results for the front surface temperatures of the PCM and the ordinary wallboards, respectively. "Expr.PCM board" and "Expr.O.board" represent the experimental results for the front surface temperatures of the PCM and the ordinary wallboards, respectively. Close agreement between the numerical and experimental results is observed from the comparisons.

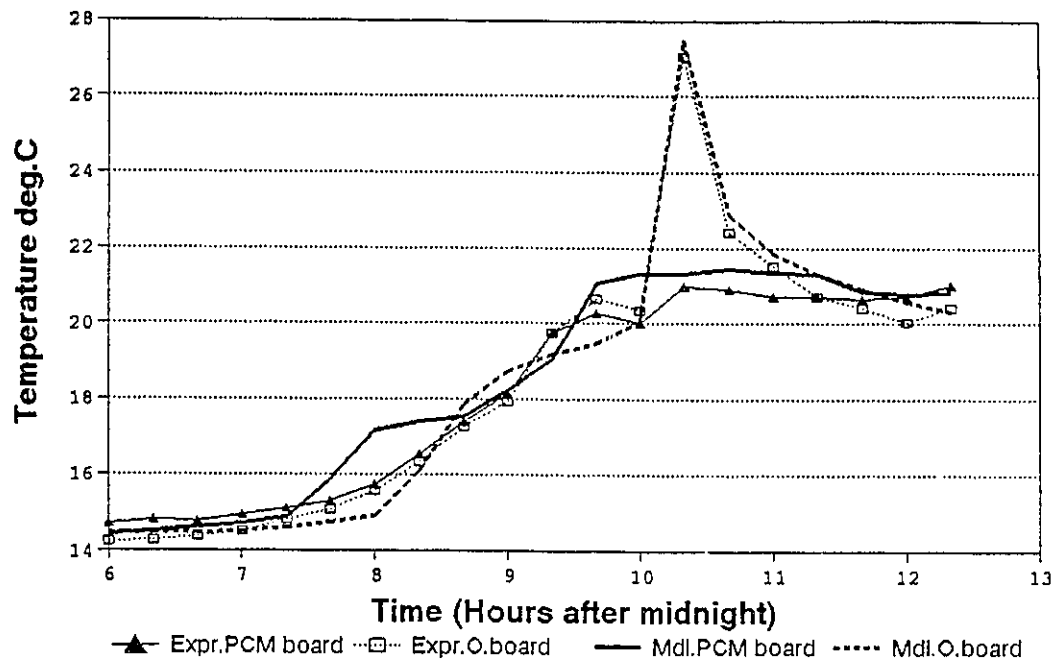
The boundary conditions of the finite difference model, which constitute the input of the program PCMBOARD, are as follows:

- 1) Inside air temperature:
 - a) constant setpoint with night setback as often used in commercial buildings, e.g. 23 °C during daytime and 16 °C during the night;
 - b) constant setpoint with night setback as used in some residential buildings, 22 °C from hour 6:00 to 22:00, and 18 °C for the rest of hours;
 - c) constant setpoint, 20 °C, without night setback, typically used for residential buildings.



The simulated experiment was performed on March 7, 1992, a cold cloudy day with lowest outside temperature -18°C ;
 Control strategy: air temperature control with $K_p=1000\text{ W/C}$, high setpoint 23°C , low setpoint 16°C , high setpoint from 6:00 to 17:00.

Figure 4.7 Comparison between the numerical and the experimental results for a freezing process, front surface temperatures of the PCM and ordinary gypsum boards



The simulated experiment was performed on March 14, 1992, a cold sunny day with lowest outside temperature -15°C and transmitted solar radiation 600 W/m^2 at noon;
Control strategy: air temperature control, $K_p=1000 \text{ W/C}$, Low setpoint $=16^{\circ}\text{C}$, high setpoint $=23^{\circ}\text{C}$, high setpoint from hour 6:00 to 17:00.

Figure 4.8 Comparison between the numerical and the experimental results for a melting process, front surface temperatures of the PCM and ordinary gypsum boards

- 2) Outside air temperature:
 - a) cold days, average $-15\text{ }^{\circ}\text{C}$;
 - b) mild days, average $-5\text{ }^{\circ}\text{C}$.
- 3) Intensity of solar radiation:
 - a) sunny days, with transmitted solar radiation between 500 to 950 W/m^2 ;
 - b) semi-cloudy days, with transmitted solar radiation between 350 to 500 W/m^2 ;
 - c) cloudy days, with transmitted solar radiation below 350 W/m^2 ;

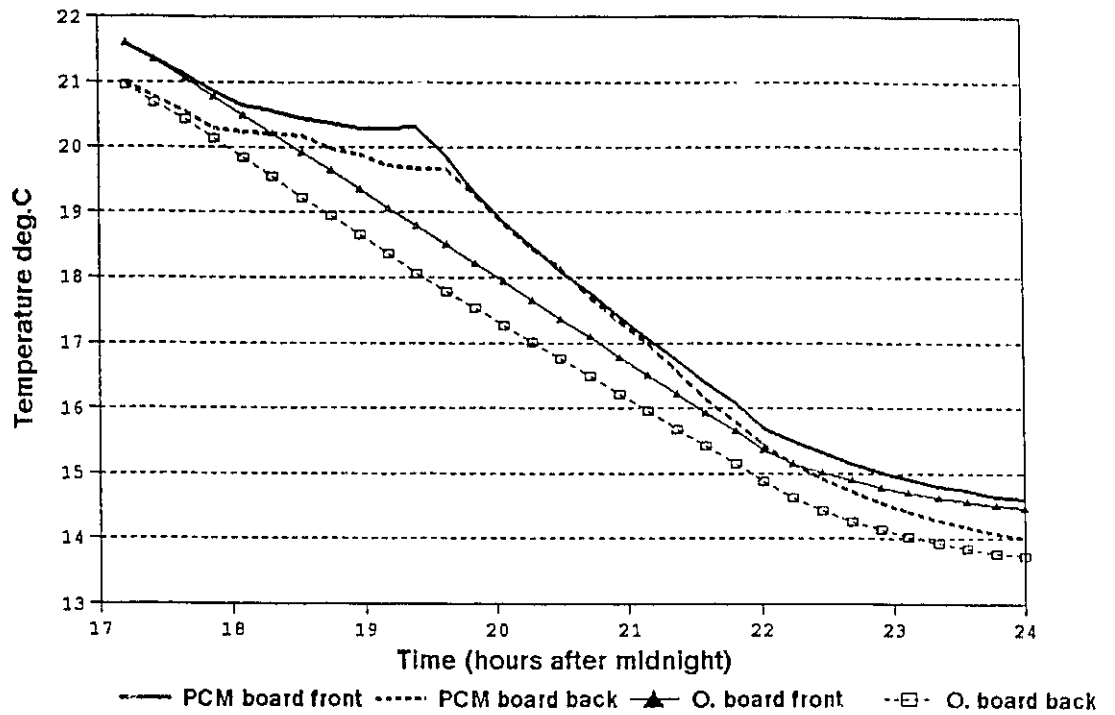
Latent heat value of the PCM gypsum board, wall structure and its thermal properties are also the information required by the program.

The outputs given by the program include:

- 1) the transient surface temperatures of the PCM and the ordinary gypsum boards;
- 2) the amount of latent heat stored or released by the PCM gypsum board.

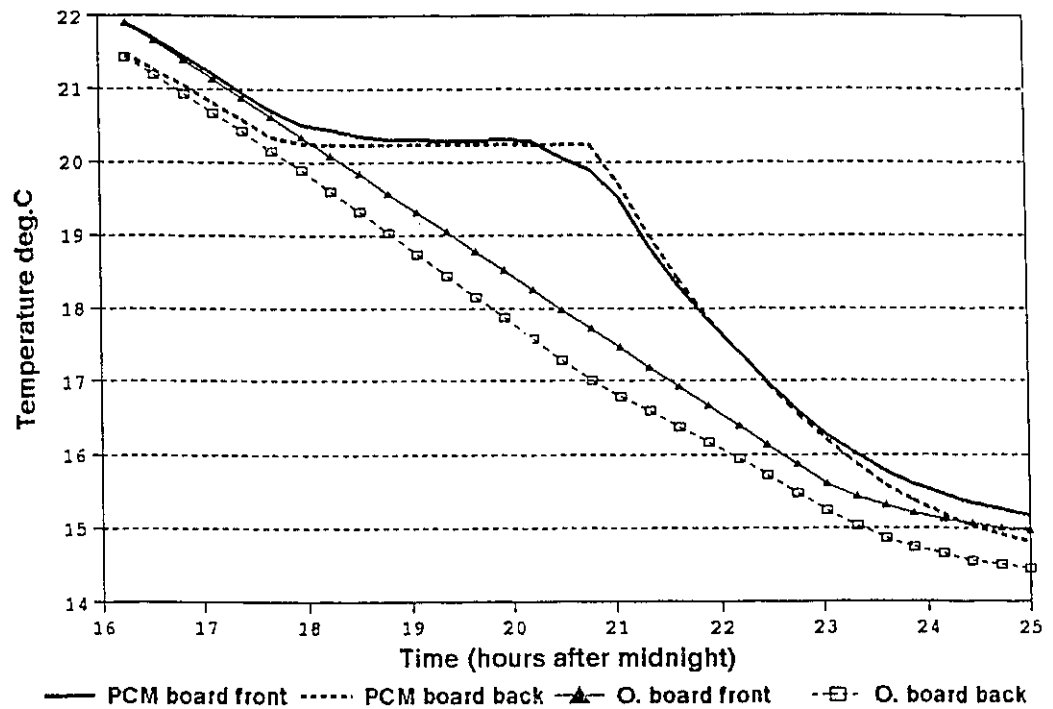
Simulations were carried out with different given inputs, such as cold/mild and sunny/cloudy weathers combined with constant setpoints with or without night setback. The simulation results are given in Figures 4.9 to 4.16.

Numerical results are generally consistent with the experimental ones. The simulation results for the melting processes, shown in Figures 4.9 and 4.10, indicate that, the average surface temperatures of the PCM wallboards are lower than the ordinary ones $4\text{-}5\text{ }^{\circ}\text{C}$ during a sunny day and $2\text{-}3\text{ }^{\circ}\text{C}$ during a cloudy day. As indicated similarly by the experimental results,



The simulation was performed for a cold cloudy day with lowest outside temperature -18°C ;
 The room air temperature was set back to 16°C from 23°C at 17:00.

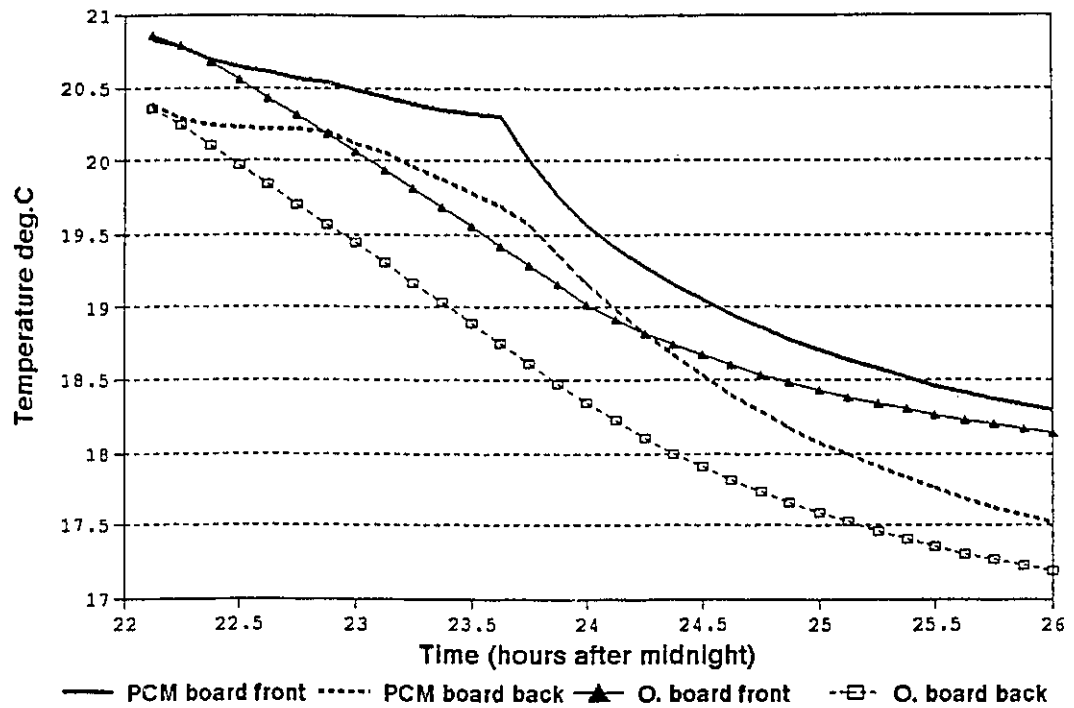
Figure 4.9 Simulation of the surface temperatures of PCM and ordinary gypsum boards
(for a freezing process during a cold sunny day with 23 to 16°C night setback)



The simulation was performed for a mild-cloudy day with lowest outside temperature -7°C ;
 The room air temperature was set back to 16°C from 23°C at 16:00.

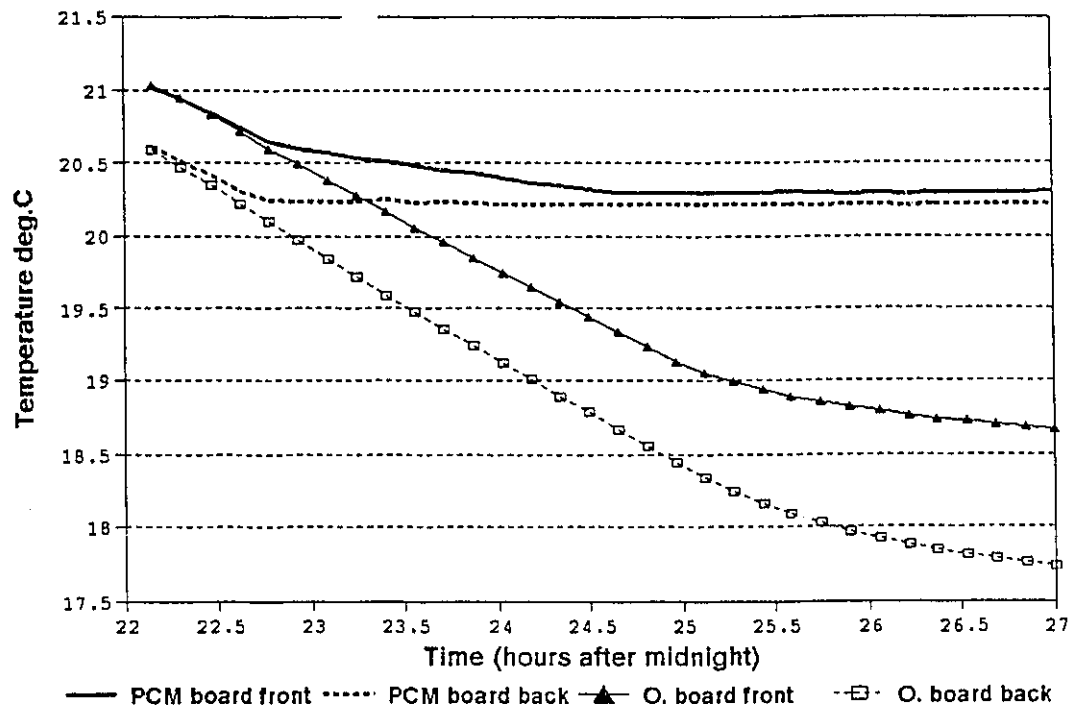
Figure 4.10 Simulation of the surface temperatures of PCM and ordinary gypsum boards

(for a freezing process during a mild cloudy day with 23 to 16 °C night setback)



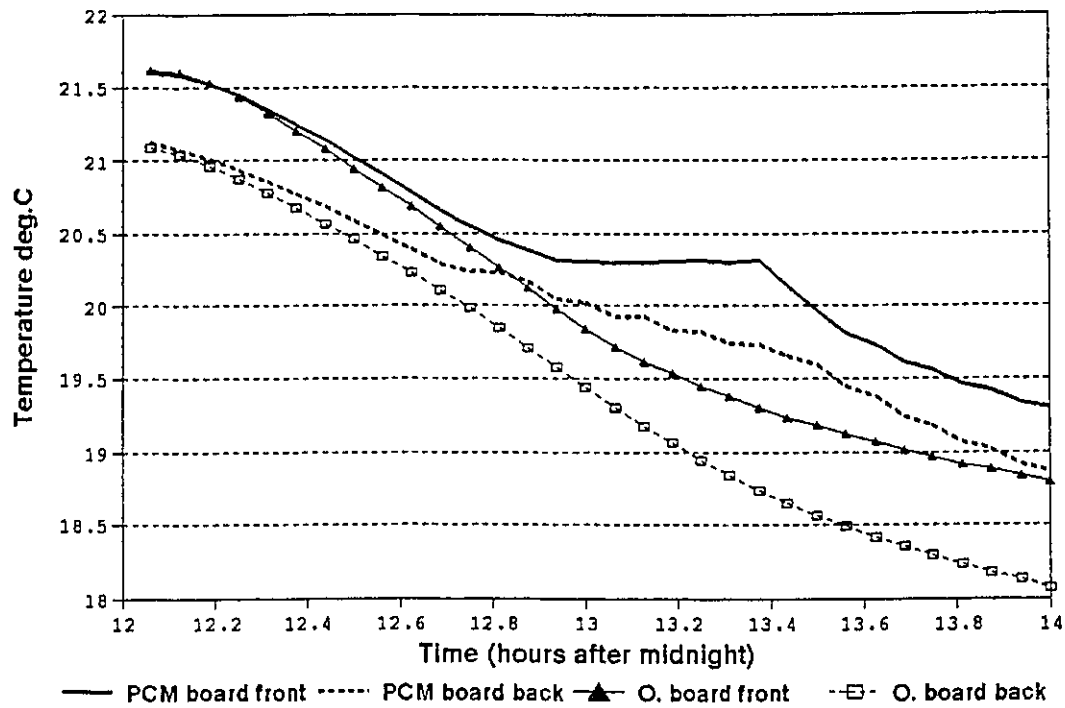
The simulation was performed for a cold-cloudy day with outside temperature -1.5°C ;
 The room air temperature was set back to 20°C from 22°C at 22:00, according to the thermal control
 strategy used for residential buildings with night setback.

Figure 4.11 Simulation of the surface temperatures of PCM and ordinary gypsum boards
(for a freezing process during a cold sunny day with 22 to 18°C night setback)



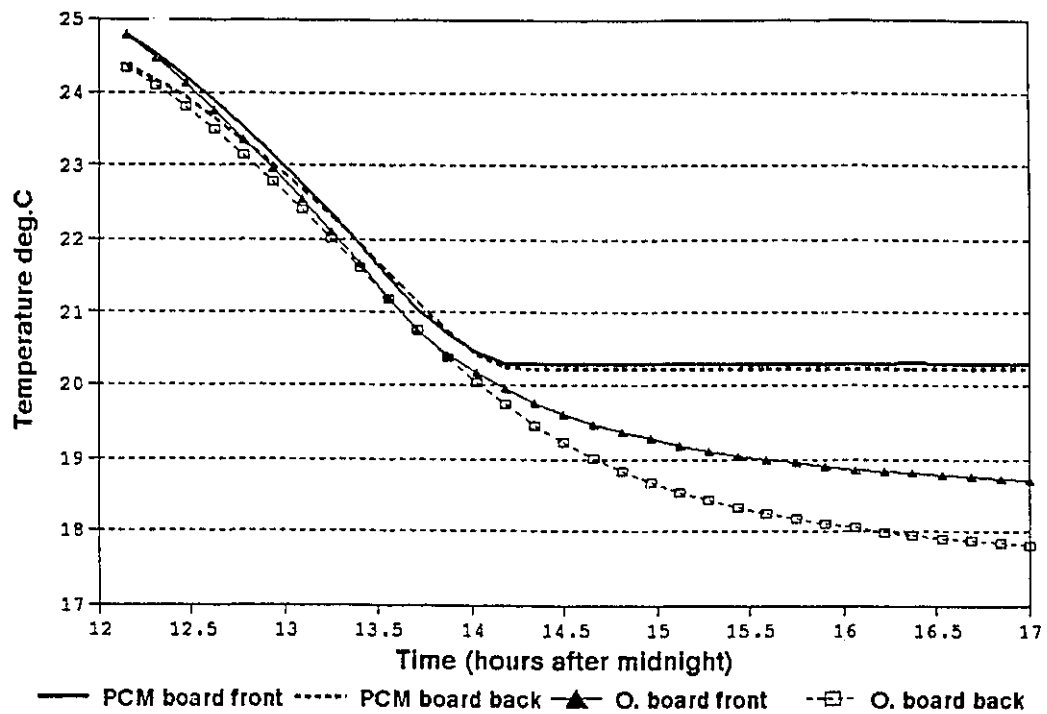
The simulation was performed for a mild winter day with outside temperature -5°C ;
 The room air temperature was set back to 20°C from 22°C at 22:00, according to the thermal control strategy used for residential buildings with night setback.

Figure 4.12 Simulation of the surface temperatures of PCM and ordinary gypsum boards
(for a freezing process during a mild sunny day with 22 to 20°C night setback)



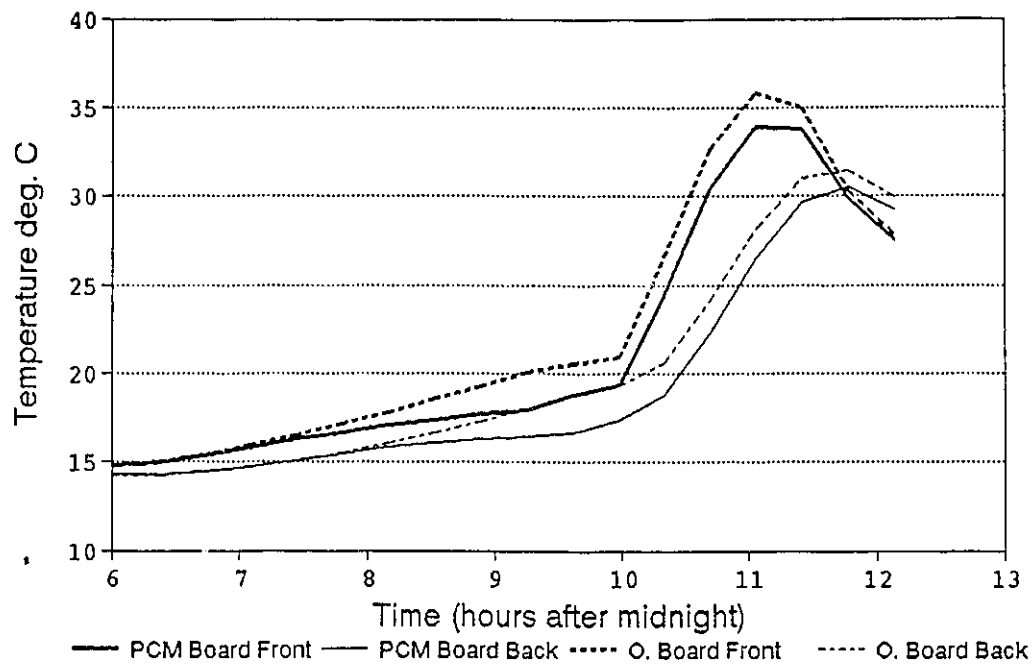
The simulation was performed for a cold sunny day with outside temperature -15°C ;
 The room air temperature was controlled at constant setpoint 20°C as in conventional residential buildings.

Figure 4.13 *Simulation of the surface temperatures of PCM and ordinary gypsum boards
 (for a freezing process during a mild sunny day with constant setpoint)*



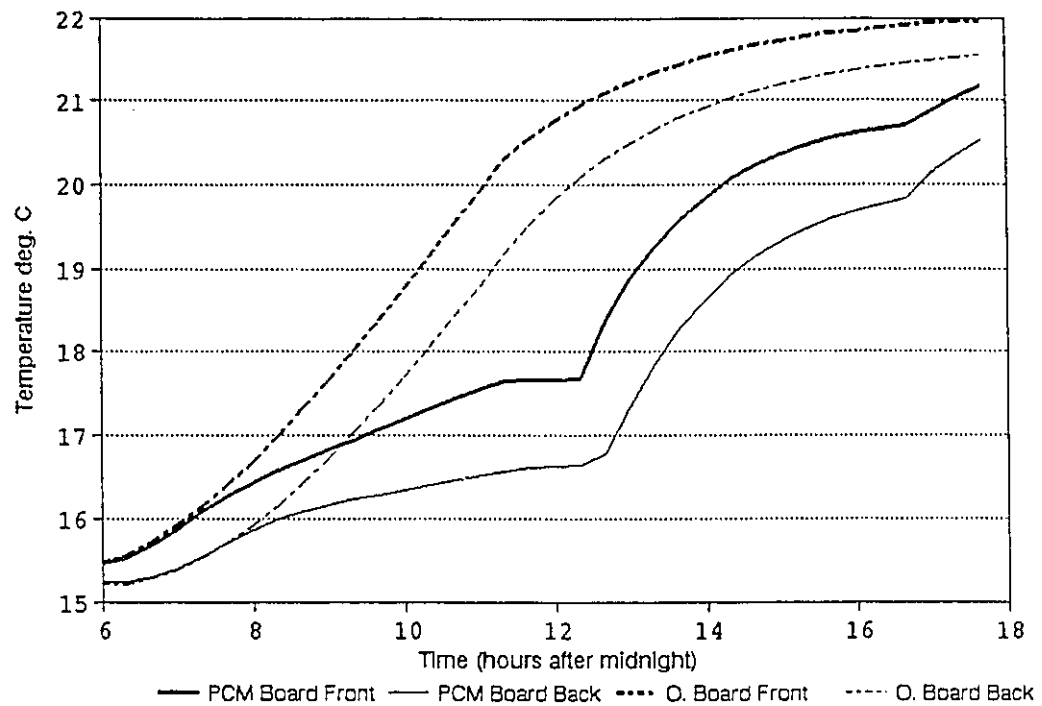
The simulation was performed for a mild sunny day with outside temperature -5°C ;
The room air temperature was controlled at constant setpoint 20°C as in conventional residential buildings.

Figure 4.14 Simulation of the surfaces temperatures of PCM and ordinary gypsum boards
(for a freezing process during a cold sunny day with constant setpoint)



The simulation was performed for a cold sunny day with outside temperature -1.6°C and transmitted solar radiation 680 W/C at noon;
 Control strategy: air temperature control, low setpoint 16°C , high setpoint 23°C , high setpoint from hour 6:00 to 17:00.

Figure 4.15 Simulation of the surfaces temperatures of PCM and ordinary gypsum boards
(for a melting process during a cold sunny day with 23 to 16 °C night setback setpoint)



The simulation was performed for a cold cloudy day with outside temperature -15°C ;
 Control strategy: air temperature control, $K_p=1000\text{ W/C}$, high setpoint $=23^{\circ}\text{C}$, low setpoint $=16^{\circ}\text{C}$,
 high setpoint from 6:00 to 17:00.

Figure 4.16 Simulation of the surfaces temperatures of PCM and ordinary gypsum boards
(for a melting process during a cold cloudy day with 23 to 16 °C night setback setpoint)

lowered PCM wallboard temperatures effectively contribute to the reduction of space overheating and the improvement of the thermal comfort. The simulation results for the freezing processes, indicate that the surface temperatures of the PCM wallboards are higher than the ordinary ones 1.5 to 2 °C for mild days (Figure 4.10) and 0.5 to 1 °C for cold days (shown in Figures 4.11 and 4.12). Figure 4.14 shows that, during a mild day when 22 to 20 °C night setback was employed (setpoint used in some residential buildings), the front surface temperature of the PCM wallboard remains almost constant at 20.2 °C for four hours. This is because the space and outside temperatures are not cool enough during the sun set and the freezing of the PCM can not be completed in a short time. Under certain thermal conditions, the PCM in the gypsum board repeats the melting and freezing cycles and the surface temperature of the PCM wallboard is maintained around the PCM's freezing point. Figures 4.15 and 4.16 show the simulation results when constant setpoint (without night setback) is used on a mild sunny day and a cold sunny day, the freezing of the PCM is realized during the sunset and the surface temperature of the PCM gypsum board is higher than the ordinary one's after the solar radiation is reduced to zero in the afternoon. As also determined from the experimental results, the higher surface temperatures of the PCM gypsum boards significantly contribute to the heating energy savings. Under various inside and outside conditions, the amount of potential energy savings by use of 1 m² of the PCM wallboard were calculated based on Equation 4.18. The results are presented in Tables 4.1-4.3.

Table 5.1 Heating power saving from the use of 1 m² BS gypsum board (23 to 16 °C night setback used)

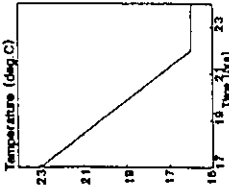
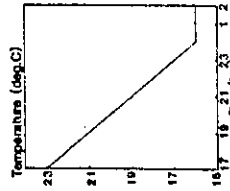
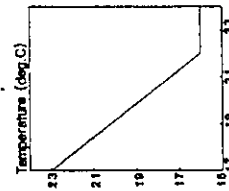
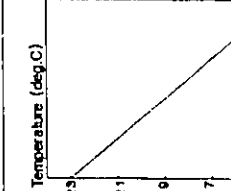
Cases	Inside temperature deg.C	Outside temperature deg.C	Energy saving Joules	Power saving W/m ²
Cold sunny day		-15	7.7x10E5	30.5
		-10 to -20	5.3x10E5	26.3
Mild sunny day		-5	2.49x10E6	69.1
		0 to -10	1.68x10E6	46.6
Cold cloudy day		-15	7.7x10E5	30.5
		-10 to -20	5.3x10E5	26.3
Mild cloudy day		0	2.49x10E6	69.1
		0 to -10	1.68x10E6	46.6

Table 5.2 Heating power saving from the use of 1 m² of BS gypsum board (22 to 18 °C night setback used)

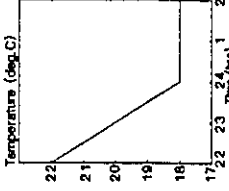
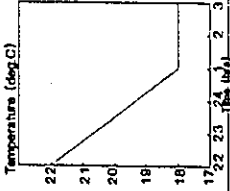
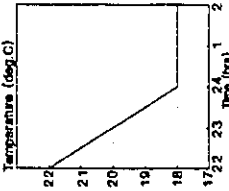
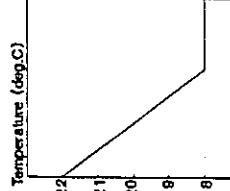
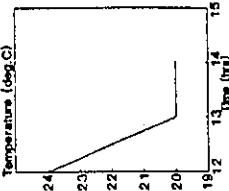
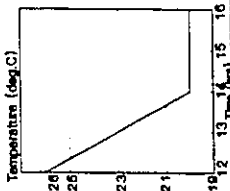
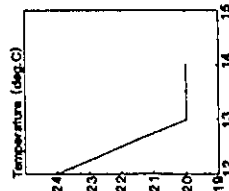
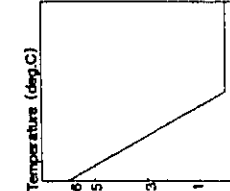
Cases	Inside temperature deg.C	Outside temperature deg.C	Energy saving Joules	Power saving W/m ²
Cold sunny day		-15	5.42x10E5	37.6
		-10 to -20	4.6x10E5	31.9
Mild sunny day		-5	1.12x10E6	62.2
		0 to -10	1.08x10E6	60.0
Cold cloudy day		-15	5.42x10E5	37.6
		-10 to -20	4.6x10E5	31.9
Mild cloudy day		0	1.12x10E6	62.2
		0 to -10	1.08x10E6	60.0

Table 5.3 Heating power saving from the use of 1 m² BS gypsum board (constant setpoint 20 °C used)

Cases	Inside temperature deg.C	Outside temperature deg.C	Energy saving Joules	Power saving W/m ²
Cold sunny day		-15	2.66x10E5	36.9
		-10 to -20	2.3610E5	32.7
Mild sunny day		-5	2,54x10E5	23.5
		0 to -10	2.28x10E5	21.1
Cold cloudy day		-15	2.66x10E5	6.96
		-10 to -20	2.3610E5	32.7
Mild cloudy day		0	2.54x10E5	23.5
		0 to -10	2.28x10E5	21.1

CHAPTER 5 CONCLUSIONS AND RECOMMENDATIONS FOR FUTURE WORK

5.1 SUMMARY

In this study, the feasibility and benefits of utilization of the PCM gypsum board in building envelope components for thermal storage were investigated. An experimental and theoretical study of the thermal performance of the PCM wallboard applied in a passive solar test-room was performed.

An experimental study was conducted in a full scale outdoor test-room with the PCM gypsum boards as its inside lining. The PCM gypsum board was made by soaking the conventional gypsum board in liquid butyl stearate, a PCM with a phase change range of 16.0 °C and 20.3 °C. The test room was equipped with a computerized data acquisition and control system for transient thermal measurements. The measurements were carried out under various weather conditions with given space setpoint temperatures.

A mathematical model, which employed an explicit finite difference procedure, was developed to simulate the transient heat transfer process in the walls with PCM gypsum board as inside lining. The model takes into account the transient boundary conditions, absorbed solar radiation, the melting/freezing of the PCM and employed a nonlinear film coefficient. The simulation of the rate of latent heat release or absorption by the PCM was based on the test results from the Differential Scanning Calorimetry (DSC), taking into account the DSC test conditions such as

the PCM's sample size and the heating/cooling rate during the test.

Based on the mathematical model, a computer model PCMBOARD was developed to conduct the computation. Reasonable agreement between the numerical and the experimental results was observed. Using the PCMBOARD, the transient thermal performance of the PCM wallboard can be analyzed and the amount of potential heating energy saving from the application of the PCM wallboard can also be calculated for various ambient and space conditions.

The main conclusions of this study are as follows:

1. Under most of the winter weather conditions, PCM gypsum board is able to act as a thermal storage device when it is used as building interior lining. The stored heat can be solar gains, excess heat from HVAC system, heat generated by occupants, lighting and appliances, etc.
2. The utilization of the PCM gypsum board in a passive solar building can reduce space temperature rise by 4-5 °C during a sunny day and thus restrict the overheating of the space. The space temperature is moderated due to the thermal storage nature of the PCM gypsum board and the space thermal comfort is improved.
3. The recovery of the stored latent heat in the PCM gypsum board can be realized when the space temperature decreases. For commercial buildings, it usually occurs when a night

setback is used in thermostatic control. For residential buildings, it usually occurs during the decrease of solar radiation or outside temperature. The recovery of the latent heat by using 1 m² of the PCM gypsum wallboard can reduce building heating load in a range of 20 to 50 watts.

4. In summary, PCM gypsum board is a promising building material in terms of the improvement of thermal comfort and energy saving for both space heating and cooling.

5.2 RECOMMENDATIONS FOR FUTURE WORK

More accurate experimental results are expected if the test is performed in two identical test-rooms, one with the PCM gypsum board installed and the other with the ordinary gypsum board installed.⁴

Presently, the model PCMBOARD is limited to the analysis of the thermal performance of a wall with the PCM gypsum board as its inside lining. In future work, the model should be extended in order to be able to determine the overall room thermal performance with PCM wallboard or other PCMs employed. The model should also be extended by conjunction with other building thermal analysis software to evaluate the design parameters for building enclosure as well as the HVAC systems.

Thermal performance of the PCM gypsum board should also be studied under summer

circumstances. Research on its application to cooling systems is also needed.

With PCM wallboard employed in the building envelope, the building operational characteristics and the HVAC system control strategies should be modified due to the change of building transfer functions.

REFERENCES

1. Anderson R. and Mehos M. (1988): "Evaluation of Indoor Air Pollutant Control Techniques Using Scale Experiments", Proc. of the ASHRAE IAQ 88, Engineering Solutions to Indoor Air Problems, pp 193-208, Atlanta, GA;
2. Douglas W. Hawes, Latent Heat Storage in Concrete, Ph.D. Thesis, 1991, Concordia University;
3. D.Feldman, D.Banu, D.Hawes and E.Ghanbari, "Obtaining an Energy Storing Building Material by Direct in Corporation of An Organic Phase Change Material in Gypsum Wallboard", Solar Energy Materials 22(1991)231-242;
4. D.Hawes, D.Banu and D.Feldman, "Latent Heat Storage in Concrete", Solar Energy Material, 19 (1989) 335-348;
5. Energy Storing Wallboard, report for Renewable Energy Branch, Energy, Mines and Resources Canada, Ottawa, Canada, DSS Contract File No.23216-6-6090/o1-ST, by Centre for Building Studies, Concordia University, 1986;
6. A.L.Berlad, "Thermal Energy Storage for Buildings", Transaction of the First International Assembly on Energy storage Held at Dubrovnik, Yugoslavia, 27 May - June, 1979;

7. A.K.Athienitis, Investigation of Thermal Storage with Floor Radiant Heating, technical report of the Centre for Building Studies, Concordia University, 1992;
8. "Thermal Properties of butyl stearate (BS) and BS gypsum board", personal contact with Dr. D. Hawes at the Centre for Building Studies, Concordia University, 1991;
9. Sami Sayegh, Mechanical and Thermal Properties of a Thermal Storage Module with Phase Change Materials Dispersed in Cement, Master Thesis, Concordia University, 1982;
10. Donald A. Neeper, "Impacts of Research Efforts on New and Existing Buildings", Los Alamos National Laboratory, LA-UR-85-869, March, 1985;
11. Donald A. Neeper, "Opportunities for Thermal Storage Research in the Solar Buildings Program", report of Los Alamos National Laboratory, Q-13:86:346S, 1986;
12. K.Peippo, P.Kauranen and P.D. Lund, "A Multi-component PCM Wall Optimized for Passive solar Heating", Energy and Buildings, 17(1991)259-270;
13. R.J.Kedl, "Wallboard with Latent Heat Storage for Passive Solar Application", ORNL/TM-11541 Distribution Category UC-202, 1991;
14. I.O.Salyer, A.K.Sircar, R.P.Chartoff and D.E.Miller, "Advanced Phase Change Materials

for Passive Solar Storage Applications", University of Dayton Research Institute, Society of Automotive Engineers, Inc., SAE/P-85/164, 1985;

15. E.V.Galen and F.J.V.Brink, "Energy Storage in Phase Change Materials for Solar Applications", International of Ambient Energy, Vol,7, No.1, January 1986;
16. A.Abhat, "Low Temperature Latent Heat Thermal Energy Storage: Heat Storage Materials", Solar Energy, Vol.30, No.4, pp 313-332, 1983;
17. A.K.Athienitis and J.Shou "Control of a Radiant Heating System Based on the Operative Temperature" ASHRAE TRANS. 1991, Vol. 97, Part 2, pp 787-794;
18. H.G.Lorsch, K.W.Kauffman and J.C.Denton, "Thermal Energy Storage for Solar Heating and Off-peak Air-conditioning", Energy Conversion, Vol.15, p.1-8;
19. J.E.Braun, "Reducing Energy Costs and Peak Electrical Demand Through Optimal Control of Building Thermal Storage", ASHRAE Transaction, 1990, Vol. 96, Part 2, pp 876-888;
20. M.N.Özisik and J.C.Uzzell, "Exact Solution for Freezing in Cylindrical Symmetry with Extended Freezing Temperature Range", Journal of Heat Transfer, 1979, Vol.101, P.331-P.334;

21. K.Morgan, "A Numerical Analysis of Freezing and Melting with Convection", Computer Method in Applied Mechanics and Engineering, 28(1981)275-284. North Holland, Publishing Company;
22. V.R.Voller and C.Prakash, "A Fixed Grid Numerical Modelling Methodology for Convection-Diffusion Mushy Region Phase Change Problems"; Int. Heat Mass Transfer, Vol.30, No.8, pp1709-1719, 1987;
23. J.C.Muehlbauer, J.D.Hatcher, D.W.Lyons and J.E.Sunderland, "Transient Heat Transfer Analysis of Alloy Solidification", ASME AICHE Heat Transfer Conference, Atlanta, GA, August 5-8, 1973;
24. Y.Cao, A.Faghri and A.Juhasz, "A PCM/Forced Convection Conjugate Transient Analysis of Energy Storage Systems with Annular and Countercurrent Flows", Journal of Heat Transfer, February 1991, Vol. 113/37;
25. J.P.Holman, Heat Transfer, 7th Edition, McGraw-Hill Publishing Company, 1990;
26. L.C.Thomas, Heat Transfer, Prentic-Hall, Inc., 1992, Englewood Cliffs, New Jersey;
27. N.B.Hutcheon, Building Science for a Cold Climate, John Wiley and Sons, 1983;

28. J.G.Shou, A Computer Technique for Heating Control Analysis and Application to Radiant Heating, Master Thesis, Concordia University, 1991;
29. ASHRAE FUNDAMENTALS, 1989, American Society of Heating, Refrigeration and Air-Conditioning Engineers, Inc, Atlanta, GA.;
30. A.K.Athienitis, C.Liu, D.Hawes, D.Banu and D.Feldman, "Investigation of the Thermal Performance of an Outdoor Test-room with Wall Latent Heat Storage", Proceedings of the 19th Annual Conference of the Solar Energy Society of Canada, 1993, Quebec;
31. "'GEN-200' Data Acquisition and Control System, Software and Hardware", 1991, Sciometric Instruments Inc., Nepean, Ontario.

Appendix-A

Data Source for the Finite Difference Model PCMBOARD

1. PCM gypsum board area

Referring to Figure 3.2 , which shows the structure of the test room, we have (unit: mm):

wall length = 3040;

wall thickness = 85;

wall width = 2400;

wall height = 2240;

door width = 900;

door height = 2030;

window width = 1219;

window height = 1219;

The total area of PCM wallboard:

$$[(3040-150) \times 2 + (2400-150) \times 2] \times 2240$$

$$- 900 \times 2030 - 1219 \times 1219$$

$$= 1.969 \times 10^7 = 19.69 \text{ m}^2$$

2. Physical and thermal properties of the PCM gypsum board used

dry weight of the ordinary gypsum board	180.016 kg
weight of the BS soaked	44.685 kg
content of the BS in the BS gypsum board	24.82 wt%

area of the BS gypsum board	19.69 m ²
thickness of the BS gypsum board	12.5 mm
density of the BS gypsum board	912.95 kg/m ³

Table A.1 Thermal properties of butyl-stearate and BS gypsum board

Material	Density Kg/m ³	Specific heat ×10 ³ J/kg.°C	Thermal conductivity W/m.°C	Phase change range °C	Latent heat J/g
Butyl stearate	855 ⁽⁴⁾	1.80 ⁽⁷⁾	0.20 ⁽⁴⁾	17.8~23 ⁽²⁾	140 ⁽²⁾
Gypsum board	720 ⁽⁷⁾	1.08 ⁽⁷⁾	0.187 ⁽⁷⁾	N/A	N/A
BS gypsum board	900 ⁽⁷⁾	1.26 ⁽⁷⁾	0.214 ⁽⁴⁾	16.5~20.9 ^(*)	30.7 ^(*)

Note: 1) numbers in brackets refer to data resources and are consistent with the ones in the references list;

2) * denotes the DSC test result from the Building Materials Labotary at the CBS, Concordia University.

3. Thermal conductivity of the wall

Referring to Figure 3.2, the thermal conductivity of the original wall(PCM gypsum board was not included) was obtained through the following calculation.

<u>Wall Components</u>	<u>Resistance °C.m²/W</u>
• inside film	omitted, it is connected to gypsum board;

- air gap between gypsum board and original wall body 0.31
 - 2×1/2" gypblock 2×0.08
 - fibreglass R12 $\times 0.176$ 2.112
 - vapour barrier 0.02
 - outside film 0.03
- $\Sigma R = 2.63$
- $U = 1/2.63 = 0.38$

4. Estimation of the thermal capacity of the wall

Two materials that consist the major thermal capacity in the wall are glass fibre and gypsum block.

- Glass fibre
 - $\rho = 8.0 \text{ lb/ft}^3$
 - $c = 0.23 \text{ Btu/(lb).}^\circ\text{F}$
 - $C = \rho \times c = 8 \times 0.23 = 1.844 \text{ Btu/ft}^3\text{C}$
 - $= 1.23 \times 10^5 \text{ J/m}^3\text{.K}$
 - thickness = 0.076m
- gypsum block
 - $\rho = 816 \text{ kg/m}^3$
 - $c = 879 \text{ J/kg.K}$
 - $C = \rho c = 7.71 \times 10^5 \text{ J/m}^3\text{.K}$
 - thickness = 0.025 mm

The thermal capacity of glass fibre and gypsum block is:

$$1.23 \times 10^5 \times 0.076 + 7.71 \times 10^5 \times 0.025 = 2.72 \times 10^4 \text{ J/K}$$

Taking into account other factors, such as steel studs, wood studs, steel lining, building paper, etc, the thermal capacity of the wall is estimated at $3.4 \times 10^4 \text{ J/K}$.

5. Nodal thermal property data for the wall considered

Referring to Figure 4.6, the thermal conductivity and heat capacity of nodes 1 to 19 are listed in Table A-1.

Table A-1 Nodal Parameters for the Explicit Finite Difference Procedure

Node		1	2	3-14	15	16	17	18	19
Conductance W/m ² .K	L	NA	10	213	213	22.5	0.88	0.8	33.3
	R	10	426	213	22.5	0.88	0.8	33.3	NA
Heat Capacity J/K		0	0	1156	1156	110000	5000	0.	0.

Appendix-B

Computer Program PCMBOARD

Computer program PCMBOARD was developed to conduct the explicit finite difference model. In this study, gypsum board with absorbed PCM, which acts as a latent heat storage device, is used as inside wall lining of an outdoor test-room. The thermal performance of the PCM gypsum board can be simulated by the computer model and the amount of energy saved by the thermal storage effect can be calculated under various given inside and outside conditions.

Inputs required by the program:

1. Thermal conductivity of PCM gypsum board, $W/m \cdot ^\circ C$;
2. Thermal conductivity of ordinary gypsum board, $W/m \cdot ^\circ C$;
3. Thermal conductance of original wall, $W/m^2 \cdot ^\circ C$;
4. Specific heat of PCM gypsum board, $J/m^3 \cdot ^\circ C$;
5. Specific heat of ordinary gypsum board, $J/m^3 \cdot ^\circ C$;
6. Thermal capacity of original wall, $J/m^2 \cdot ^\circ C$;
7. Initial inside and outside air temperatures;
8. Parameters with respect to inside and outside air temperature variations vs time. Referring to Figure-15, these parameters include different values for inside and outside temperatures $TI1, TI2, TI3, TO1, TO2, TO3, TO4$ and the different values indicate the time period $tpI1, tpI2, tpO1, tpO2, tpO3$, etc.
9. Latent heat value of PCM gypsum board, J/kg .

Output from the program:

1. The benefit gained from the thermal storage of PCM gypsum board, Watts. It is equivalent to the extra amount of heat exchange between wall and inside ambient due to the utilization of PCM gypsum board instead of use of ordinary gypsum board.
2. The increase of thermal storage due to the utilization of PCM gypsum board instead of ordinary gypsum board.

Appendix C

Determination of Inside Film Coefficient

It is important not to ignore radiative heat transfer in the calculation of total heat loss or gain. Refer to [24] and [26], the heat transfer coefficient, f_{in} , between the gypsum board surface and inside air is :

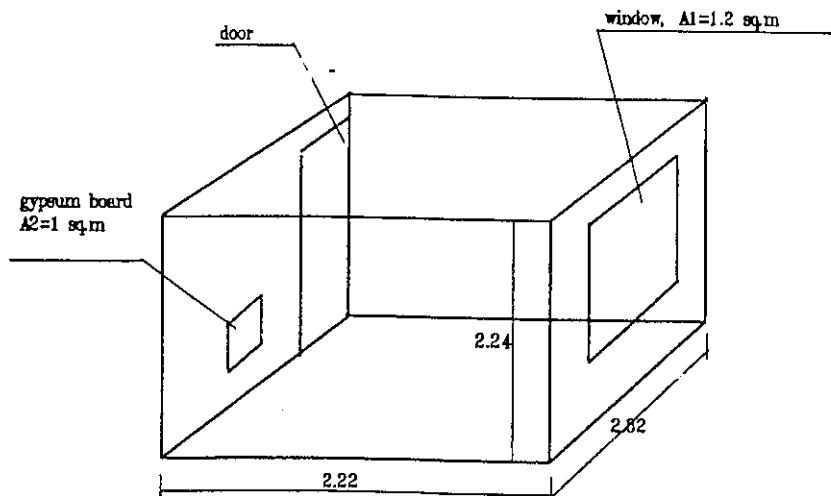
$$f_{in} = h_r + h_c$$

where, h_r = radiative heat transfer coefficient,

h_c = natural convective heat transfer coefficient.

h_r

Referring to the figure below, the angle factor $F_{A2-A1} = 0.1$.



A_1 is the window area (1.2 m^2). A_2 denotes the concerned gypsum board (1 m^2). A_3 denotes the rest of the inside room surface beside the window.

$$h_r = F_{A2-A1} h_{r_{A2-A1}} + (1-F_{A2-A1}) h_{r_{A2-A3}}$$

$$h_r = \sigma \epsilon [F_{A2-A1} T_1^3 + (1-F_{A2-A1}) \frac{T_1^4 - T_3^4}{T_1 - T_3}]$$

h_c

For a large vertical surface, the convective heat transfer coefficient is:

$$h_c = 1.31 (\Delta T)^{1/3}$$